

# Formation Control of Networked Mobile Robots With Unknown Reference Orientation

Jianing Zhao , *Student Member, IEEE*, Keyi Zhu, Hanjiang Hu, Xiao Yu , *Member, IEEE*, Xianwei Li, *Member, IEEE*, and Hesheng Wang , *Senior Member, IEEE*

**Abstract**—In this article, the distributed leader-following formation control problem of networked mobile robots is investigated. The desired formation is specified by a reference trajectory generated by the leader and the followers' desired relative positions with respect to the leader. On the one hand, for any security-aware multirobot systems, the values of the leader's position and orientation are generally not allowed to be transmitted via the inter-robot communication in the case of the information leakage of formation caused by the possible eavesdropping. On the other hand, relative orientations, different from relative positions, are typically difficult for mobile robots to measure directly, which makes the reference orientation unknown to all followers. In order to track the reference trajectory and form a desired formation in the absence of the reference orientation, followers are divided into two groups according to whether they are able to directly measure the relative positions with respect to the leader. The topology of the sensing/communication network among multirobot systems is described by a directed graph containing a directed spanning tree. Then, two observer-based control laws are proposed for two groups of followers, respectively, in both of which the unknown tracking errors are properly estimated. It is rigorously proven that the resulting closed-loop multirobot system is globally uniformly asymptotically stable. Finally, the effectiveness of our approach is illustrated by

an experiment conducted on networked TurtleBot3 Burger mobile robots.

**Index Terms**—Autonomous robots, control of robotic networks, distributed control, formation control, multiagent control systems, synchronization.

## I. INTRODUCTION

THE formation control of multirobot systems has attracted tremendous research attention in recent years due to its wide applications in both civilian and military fields; see [1], [2], [3], [4], [5], and references therein. Existing approaches to tackle the formation control problem of mobile robots can be categorized into behavior-based [6], virtual-structure [7], and leader-following schemes [8]. In particular, the leader-following one is adopted to track a physical target with the motion information known or partially known, which is described as “leader”. The objective of the leader-following formation control is to make all followers track an autonomous leader and maintain a desired geometric structure with respect to the leader. If the mobile robots are simply modeled as single-integrators or double-integrators, the broad existing results on the leader-following consensus of multiagent systems, for example, [9], can be applied or generalized to the formation control problems, as in [10], [11], and [12]. However, the orientation is an important state for a real mobile robot, which needs to be considered in the system model together with the nonholonomic motion constraint.

The unicycle model takes both the orientation and the nonholonomic constraint of a mobile robot into consideration. Many existing works focused on the formation control problems of unicycle-type mobile robots. In [13], a framework based on graph theory was first developed for the modeling and control of multiple unicycle-type mobile robots. Based on this framework, the Lyapunov stability analysis of a static formation under distributed control laws was presented in [14]. A nonlinear control approach for mobile robots modeled by dynamic unicycles with inter-robot communication was proposed in [15]. Besides, many formation control problems concerning some practical issues have been investigated. In [16], [17], [18], [19], and [20], the formation tracking problems of mobile robots subject to velocity or curvature constraints were studied. In [21], a receding-horizon controller to improve the convergence performance of formation tracking errors was developed. The relaxed persistency of

Manuscript received 1 August 2022; revised 17 October 2022; accepted 18 December 2022. Date of publication 20 January 2023; date of current version 16 August 2023. Recommended by Technical Editor J. Yang and Senior Editor K. J. Kyriakopoulos. This work was supported in part by the National Key R&D Program of China under Grant 2021ZD0112600, in part by the Funds of the National Natural Science Foundation of China under Grant 62173283, Grant 61803262, Grant 61903250, Grant 61722309, and Grant U1613218, and in part by the Foundation of Key Laboratory of System Control and Information Processing, the Ministry of Education, China. (Corresponding author: Xiao Yu.)

Jianing Zhao, Keyi Zhu, Xianwei Li, and Hesheng Wang are with the Department of Automation, Shanghai Jiao Tong University, Shanghai 200240, China, and also with the Key Laboratory of System Control and Information Processing, Ministry of Education of China, Shanghai 200240, China (e-mail: jnzhao@sjtu.edu.cn; bai12wp@alumni.sjtu.edu.cn; xianwei.li@sjtu.edu.cn; wanghesheng@sjtu.edu.cn).

Hanjiang Hu is with the Department of Mechanical Engineering, Carnegie Mellon University, Pittsburgh, PA 15213 USA (e-mail: huhanjiang@cmu.edu).

Xiao Yu is with the Department of Automation, Xiamen University, Xiamen 361005, China, and also with the Key Laboratory of System Control and Information Processing, Ministry of Education of China, Shanghai 200240, China (e-mail: xiaoyu@xmu.edu.cn).

This article has supplementary material provided by the authors and color versions of one or more figures available at <https://doi.org/10.1109/TMECH.2022.3231079>.

Digital Object Identifier 10.1109/TMECH.2022.3231079

excitation condition in formation tracking control was considered in [22]. More recently, a vision-based adaptive technique has been developed in [23] to achieve formation control, assuming that the velocity of the leader was constant and unknown. However, it was assumed in all aforementioned works that both the position of the leader and the reference orientation have to be available to at least one follower, either by measurement or by communication, so as to achieve a formation defined by a desired position and the synchronized orientation.

Nevertheless, rather than the leader's real-time position, it is more difficult for the followers to obtain the reference orientation in practice. To be specific, there are a number of sensing devices, for example, the LiDAR, camera, sonar, etc., to directly measure the relative positions between a pair of neighboring robots, while the main means of sensing relative orientations are vision-based, including the line-of-sight measurements [24], [25] and the pan-camera-unit measurements [26], [27]. To this end, the existing formation control approaches depending on the relative orientation measurements become much restricted when there is a vision-denied scenario, like the underwater environment or the night environment. The wireless communication is an alternative way to obtain the reference orientation, that is, the leader measures its own orientation and transmits it to the followers via communication as in [15] and [22]. However, for any security-aware multirobot systems, the information transmitted via the communication channels is vulnerable to be eavesdropped by the adversary, which is typically common in the military application of formation control. Moreover, the information of leader's position and orientation is generally the most important privacy of multirobot systems, since the position concerns the safety of multirobot systems and the orientation may reveal the destination of the formation. Therefore, it is also not applicable for the followers to obtain the reference orientation when the security is taken into consideration.

The aforementioned issues motivate the study on the control of mobile robots with unknown reference orientation. In [28], an observer-based control law was developed to solve the trajectory tracking problem of one single robot without reference orientation, and the local stability of the closed-loop system was established. Based on this result, a tracking controller with the orientation error observer was proposed and applied to the vehicle platooning problem in [29]. Nevertheless, only one single robot was taken into account in [28], and the multirobot systems with the network topology being a simple chain were considered in [29]. Therefore, we are motivated to solve the leader-following formation tracking control problem for multirobot systems with a general network topology, in the case where the reference orientation is unknown to all followers.

In this article, the topology of the sensing and communication network underlying multirobot systems is described by a directed graph containing a directed spanning tree. The reference trajectory is generated by the leader, and the reference driving and steering velocities are known to all followers by the broadcast from the leader. Followers are divided into two groups based on whether they could directly sense the leader, i.e., whether the leader is one of their neighbors in the graph. Two dynamic controllers are designed, respectively, for these two groups

depending on the relative position measurements, while neither the reference orientation nor relative orientation measurements are required. Note that both of the leader's position and orientation are not transmitted via the communication channels in the case of the information leakage of the formation's privacy. We establish the global asymptotic stability of the resulting closed-loop multirobot system, based on a technical lemma on sufficient conditions of uniform exponential/asymptotic stability for a nonlinear perturbed system. Finally, an experiment on networked TurtleBot3 Burger mobile robots is shown to validate the effectiveness of the proposed control approach.

The main contributions of this article are twofold. First, the proposed distributed control laws for formation tracking do not rely on the reference orientation any more, which contrasts most of the existing works on the formation control of nonholonomic robots; see, for instance, [13], [14], [16], [17], [18], [19], [20], [21], [22], and [23]. This setting is more reasonable especially when multirobot systems are security aware and the vision-based sensing devices are denied. Second, compared with [28] and [29], which also considered the absence of reference orientation, our approach exhibits its merit. It is noted that the trajectory tracking of only one single robot was studied in [28] and that vehicle platooning with the simple chain topology was investigated in [29]. In contrast, this article considers the multirobot systems with a more complex network topology described by a directed graph containing a spanning tree, which includes the cases in [28] and [29] as special cases. Moreover, different from [28] and [29] where the initial orientations of followers are confined to an interval, our design leads to the global uniform asymptotic stability of the resulting closed-loop system, which renders no limitation on both initial positions and orientations of the followers.

The rest of this article is organized as follows. In Section II, the problem formulation and some necessary preliminaries are presented. In Section III, the main results, including control law design and stability analysis, are explicitly given. In Section IV, the laboratorial experimental results are shown. Finally, Section V concludes this article.

*Notations and definitions:*  $|\cdot|$  is the absolute value of a scalar. For a vector  $\mathbf{x} = [x_1, \dots, x_n]^T \in \mathbb{R}^n$ , the Euclidean norm  $\|\cdot\|$  is defined as  $\|\mathbf{x}\| = \sqrt{\mathbf{x}^T \mathbf{x}}$ .

## II. PRELIMINARIES AND PROBLEM FORMULATION

### A. Problem Formulation

Consider a group of  $N + 1$  nonholonomic mobile robots. For  $i = 0, 1, \dots, N$ , the kinematics of robot  $i$  is described by

$$\dot{x}_i = v_i \cos \theta_i, \quad \dot{y}_i = v_i \sin \theta_i, \quad \dot{\theta}_i = \omega_i \quad (1)$$

where  $\mathbf{p}_i = [x_i, y_i]^T \in \mathbb{R}^2$  represents the Cartesian coordinates of the position of robot  $i$ , and  $\theta_i \in \mathbb{R}$  is the heading angle pointing to the robot's orientation in the global coordinate frame.  $v_i \in \mathbb{R}$  and  $\omega_i \in \mathbb{R}$  are the driving and steering velocities, respectively. In particular, the reference trajectory for the multirobot system, indexed by  $i = 0$ , i.e.,  $[x_0(t), y_0(t), \theta_0(t)]^T$ ,

is generated by the leader with the following kinematics:

$$\dot{x}_0 = v_r \cos \theta_0, \quad \dot{y}_0 = v_r \sin \theta_0, \quad \dot{\theta}_0 = \omega_r \quad (2)$$

where  $v_r$  and  $\omega_r$  are the reference driving and velocities broadcast from the leader to the multirobot system. Moreover, the reference velocities satisfy the following assumption, which is widely used in the trajectory tracking and formation control; see, for example, [22] and [28].

*Assumption 1:*  $v_r(t)$  is bounded and  $\omega_r(t)$  is persistently exciting for all  $t \geq t_0$ .

The aim of this article is to achieve the formation control of the multirobot system through the distributed sensing and communication among the robots. The topology of the sensing and communication network is described by a directed graph  $\mathcal{G} = (\mathcal{V}, \mathcal{E}, \mathcal{A})$ , where  $\mathcal{V}$  is the node set containing all mobile robots, the edge set  $\mathcal{E} = \{(j, i) : j \neq i, i, j \in \mathcal{V}\}$  contains the directed edges from node  $j$  to node  $i$ , and  $\mathcal{A} = [a_{ij}] \in \mathbb{R}^{N \times N}$  is the weighted adjacency matrix, with  $a_{ij} > 0$  if  $(j, i) \in \mathcal{E}$ ; otherwise,  $a_{ij} = 0$ . Denote the set of neighbors of robot  $i$  as  $\mathcal{N}_i = \{j \in \mathcal{V} : (i, j) \in \mathcal{E}\}$ . A directed edge  $(j, i)$  represents that some information of robot  $j$  is available to robot  $i$  via sensing or communication. The Laplacian matrix is defined as  $\mathcal{L} = [l_{ij}] \in \mathbb{R}^{N \times N}$  with  $l_{ij} = -a_{ij}$  if  $j \neq i$ , and  $l_{ij} = \sum_{j=1}^N a_{ij}$  if  $j = i$ . Besides, to describe the interaction between each follower and the leader, we introduce a nonnegative matrix  $\mathcal{B} = \text{diag}(b_i)$ , with  $b_i = 1$  if  $(0, i) \in \mathcal{E}$  and otherwise  $b_i = 0$ . Finally, define

$$\mathcal{H} = \mathcal{L} + \mathcal{B}. \quad (3)$$

As a fundamental assumption on control of multirobot systems, the following assumption is required.

*Assumption 2:* The directed graph  $\mathcal{G}$  contains a directed spanning tree, in which the leader node 0 is the root with no incoming edges.

The desired formation of the multirobot system is defined by the desired relative position of each follower  $i$  with respect to the leader, denoted by  $\mathbf{d}_{i0} = [d_{i0}^x, d_{i0}^y]^T$ . However, since not all robots have the information of the leader, the desired formation is equivalently specified by the desired relative positions for each pair of neighboring robots  $(i, j) \in \mathcal{E}$ , i.e.,  $\mathbf{d}_{ij} = [d_{ij}^x, d_{ij}^y]^T$ , with  $\mathbf{d}_{ij} = \mathbf{d}_{i0} - \mathbf{d}_{j0}$ . Meanwhile, the synchronized orientations of all robots are also required in the desired formation. That is, the objective of the leader-following formation tracking control is to make all followers converge to those desired positions, i.e., make  $x_0 - x_i \rightarrow d_{i0}^x$ , and  $y_0 - y_i \rightarrow d_{i0}^y$ , and the same orientation as the reference one, i.e.,  $\theta_0 - \theta_i \rightarrow 2K_i\pi$  with some  $K_i \in \mathbb{Z}$ .

To solve a formation tracking problem, the tracking errors are generally defined in the global coordinate frame as

$$e_i^x = x_0 - x_i + d_{i0}^x, \quad e_i^y = y_0 - y_i + d_{i0}^y, \quad e_i^\theta = \theta_0 - \theta_i. \quad (4)$$

Considering the fact that  $\theta_i$  and  $\theta_i + 2K_i\pi$ ,  $K_i \in \mathbb{Z}$ , represent the same orientation, it is not necessary to use the true value of  $\theta_i$  for the design of control laws. Then, we define

$$s_i = \sin \theta_i, \quad c_i = \cos \theta_i \quad (5)$$

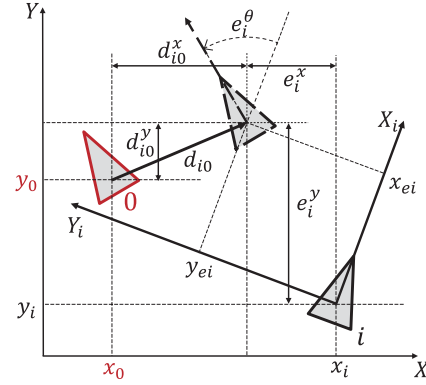


Fig. 1. Illustration for the tracking errors: the leader and the follower are represented by the red robot and the black robot (with solid-line edge) respectively, and the black robot (with dashed-line edge) denotes the desired position and orientation of the follower.

and transform (1) to a new kinematic model as

$$\begin{bmatrix} \dot{x}_i \\ \dot{y}_i \\ \dot{s}_i \\ \dot{c}_i \end{bmatrix} = \begin{bmatrix} c_i & 0 \\ s_i & 0 \\ 0 & c_i \\ 0 & -s_i \end{bmatrix} \begin{bmatrix} v_i \\ \omega_i \end{bmatrix}. \quad (6)$$

Besides, the origin of the global coordinate frame is also unknown to the multirobot system, and the robots rely on their relative positions. Accordingly, we convert the position tracking errors (4) using the following transformation [30]:

$$\begin{bmatrix} x_{ei} \\ y_{ei} \end{bmatrix} = \begin{bmatrix} c_i & s_i \\ -s_i & c_i \end{bmatrix} \begin{bmatrix} e_i^x \\ e_i^y \end{bmatrix} \quad (7)$$

and introduce two new orientation tracking errors as

$$s_{ei} = \sin e_i^\theta, \quad c_{ei} = 1 - \cos e_i^\theta. \quad (8)$$

Thus, to achieve the desired formation, it suffices to make the tracking errors  $[x_{ei}, y_{ei}, s_{ei}, c_{ei}]^T$  converge to zero. The above tracking errors are illustrated in Fig. 1.

In this article, it is supposed that the leader is autonomous and collaborative to the followers. Under Assumption 2, there exists at least one follower robot, which is able to detect or identify the leader. Thus, followers can be divided into two groups, denoted by  $\mathcal{V}_A = \{1, \dots, n_A\}$ ,  $n_A \geq 1$  and  $\mathcal{V}_B = \{n_A + 1, \dots, N\}$ . Each follower in  $\mathcal{V}_A$  could sense the leader, and thus, the relative position with respect to the leader is assumed to be measured, while all followers in  $\mathcal{V}_B$  do not know the leader and do not have access to any state of the leader. Note that the followers in the two groups have different specifications and, thus, undertake different tasks in the formation control. To this end, we need to design the control laws for the two groups, respectively. Similar to the follower in  $\mathcal{V}_A$ , each follower in  $\mathcal{V}_B$  is able to measure the relative positions to its neighbors. Note that the desired positions, including  $[d_{i0}^x, d_{i0}^y]^T$  and  $[d_{ij}^x, d_{ij}^y]^T$ , are defined in the presence of a common sense of direction. Thus, all followers need to share a reference for direction, and each one measures its own

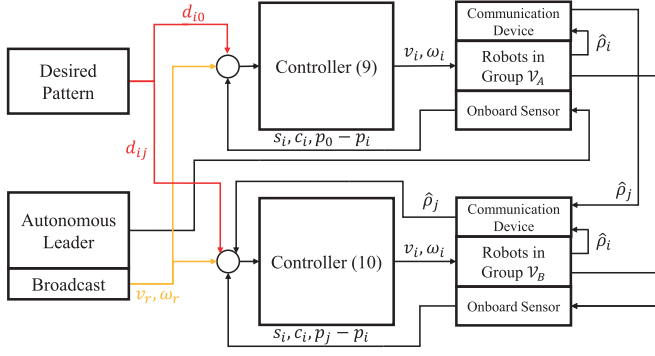


Fig. 2. Diagram of the problem formulation for Problem 1.

orientation. The available measurements to followers are stated in the following assumption.

*Assumption 3:* Each follower  $i$  has access to its own orientation  $[s_i, c_i]^T$ . Follower  $i$ ,  $i \in \mathcal{V}_A$ , measures the relative position  $[x_0 - x_i, y_0 - y_i]^T$ , while follower  $i$ ,  $i \in \mathcal{V}_B$ , measures the relative positions  $[x_j - x_i, y_j - y_i]^T$ ,  $j \in \mathcal{N}_i$ .

Now, the formation control of mobile robots with unknown reference orientation is formulated as follows, while a corresponding block diagram is provided in Fig. 2.

*Problem 1:* Consider  $N + 1$  nonholonomic robots with kinematics (1) and a network topology described by the graph  $\mathcal{G}$ . Given the reference velocities  $[v_r, \omega_r]^T$ , and the desired formation specified by the desired relative positions  $\mathbf{d}_{i0} = [d_{i0}^x, d_{i0}^y]^T$ ,  $i \in \mathcal{V}_A$  and  $\mathbf{d}_{ij} = [d_{ij}^x, d_{ij}^y]^T$ ,  $(i, j) \in \mathcal{E}$ :

- 1) for follower  $i \in \mathcal{V}_A$  with any initial states  $[e_i^x(t_0), e_i^y(t_0), e_i^\theta(t_0)]^T \in \mathbb{R}^3$ , design a dynamic control law in form of

$$\begin{aligned} [v_i, \omega_i]^T &= \sigma_A(\hat{\rho}_i, s_i, c_i, v_r, \omega_r, \mathbf{p}_0 - \mathbf{p}_i, \mathbf{d}_{i0}) \\ \dot{\hat{\rho}}_i &= \varrho_A(\hat{\rho}_i, s_i, c_i, v_r, \omega_r, \mathbf{p}_0 - \mathbf{p}_i, \mathbf{d}_{i0}) \end{aligned} \quad (9)$$

- 2) for follower  $i \in \mathcal{V}_B$  with any initial states  $[e_i^x(t_0), e_i^y(t_0), e_i^\theta(t_0)]^T \in \mathbb{R}^3$  and follower  $j \in \mathcal{N}_i$  being its neighbor, design a dynamic control law in form of

$$\begin{aligned} [v_i, \omega_i]^T &= \hat{\rho}_B(\rho_i, s_i, c_i, v_r, \omega_r, \mathbf{d}_{ij}) \\ \dot{\hat{\rho}}_i &= \varrho_B(\hat{\rho}_i, \hat{\rho}_j, s_i, c_i, v_r, \omega_r, \mathbf{p}_j - \mathbf{p}_i, \mathbf{d}_{ij}) \end{aligned} \quad (10)$$

such that

$$\lim_{t \rightarrow \infty} [x_{ei}, y_{ei}, s_{ei}, c_{ei}] = \mathbf{0}, \quad i \in \mathcal{V}_A \cup \mathcal{V}_B \quad (11)$$

where  $\mathbf{p}_j - \mathbf{p}_i$  are the relative positions,  $\hat{\rho}_i$  and  $\hat{\rho}_j$  are internal states of the follower robots  $i$  and  $j$ , respectively, to be designed for the orientation estimation, and  $\sigma_A(\cdot)$ ,  $\varrho_A(\cdot)$ ,  $\sigma_B(\cdot)$ , and  $\varrho_B(\cdot)$  are sufficiently smooth functions.

*Remark 1:* In Problem 1, we adopt the setting, as in [18], [19], [22], [28], and [29], that the reference driving and steering velocities  $v_r$  and  $\omega_r$  are known to the multirobot system. In practice,  $v_r$  and  $\omega_r$  are broadcast from the leader to all followers, which is conducive to the smooth implementation of the task. Instead, it is noted that the transmission of leader's position and orientation is not allowed in Problem 1 due to

the consideration for security. When it refers to the application of formation control, especially in the military field, different from the reference velocities, the information of the leader's position and orientation is generally the most important privacy of any security-aware multirobot systems whose communication channel is vulnerable to be eavesdropped by the adversary. That is, if the position information were leaked, the multirobot system could be attacked by the adversary; if the orientation information were leaked, the destination of the multirobot system's mission might be exposed.

*Remark 2:* It is obvious in Problem 1 that neither the reference orientation  $\theta_0$  nor the relative orientations including  $\theta_0 - \theta_i$  and  $\theta_j - \theta_i$  are required, while the information of  $\theta_0$  is needed in [15], [18], [19], [20], and [22] and the measurements of  $\theta_0 - \theta_i$  and  $\theta_j - \theta_i$  are utilized in [23]. This is motivated by the fact that the relative orientation is typically difficult for the mobile robots to directly measure in practice, especially in the vision-denied scenario, given that the transmission of reference orientation by communication is not allowed. Take the underwater workspace as an example. It is rather difficult for sonar, the most important sensing equipment of underwater robots, to directly measure the orientation of other robots or relative orientation with respect to others. Even though for the ground or aerial vehicles, the accurate measurement of relative orientations also brings high requirements on sensors as well as inevitable large noise. Therefore, it is highly significant for us to treat the position and orientation differently.

## B. Technical Lemmas

Before the main results are presented, we present three technical lemmas, which are used in the following section.

First, motivated by the cascaded system theory [31], we provide a technical lemma to stabilize a perturbed system exponentially or asymptotically. The detailed proof is given in Appendix A.

*Lemma 1:* Consider a perturbed system

$$\dot{\mathbf{z}} = \mathbf{f}(t, \mathbf{z}) + \mathbf{g}(t, \mathbf{z}, \boldsymbol{\psi}) \quad (12)$$

where  $\mathbf{z} \in \mathbb{R}^{n_z}$  is the state and  $\boldsymbol{\psi} \in \mathbb{R}^{n_\psi}$  is an exogenous signal. Functions  $\mathbf{f}(t, \mathbf{z})$  and  $\mathbf{g}(t, \mathbf{z}, \boldsymbol{\psi})$  are piecewise continuous in  $t$  and locally Lipschitz in  $\mathbf{z}$  and  $(\mathbf{z}, \boldsymbol{\psi})$ , respectively. System (12) can be viewed as a nominal system

$$\dot{\mathbf{z}} = \mathbf{f}(t, \mathbf{z}) \quad (13)$$

with a perturbation  $\mathbf{g}(t, \mathbf{z}, \boldsymbol{\psi})$ . Let  $\mathbf{z} = \mathbf{0}$  be an equilibrium of the nominal system (13), and  $\mathcal{Z} \subset \mathbb{R}^{n_z}$  be a domain containing  $\mathbf{z} = \mathbf{0}$ . System (13) is uniformly exponentially stable for  $\mathbf{z} \in \mathcal{Z}$ , and  $\mathbf{g}(t, \mathbf{z}, \boldsymbol{\psi})$  satisfies

$$\|\mathbf{g}(t, \mathbf{z}, \boldsymbol{\psi})\| \leq b_1 \|\boldsymbol{\psi}\| \|\mathbf{z}\| + b_2 \|\boldsymbol{\psi}\| \quad (14)$$

with two positive constants  $b_1$  and  $b_2$ . Then, system (12) is:

- a) uniformly exponentially stable if  $\boldsymbol{\psi}(t)$  converges to  $\mathbf{0}$  exponentially as  $t \rightarrow \infty$ ;
- b) uniformly asymptotically stable if  $\boldsymbol{\psi}(t)$  converges to  $\mathbf{0}$  asymptotically as  $t \rightarrow \infty$ ;

c) uniformly exponentially stable if  $\mathbf{g}(t, \mathbf{z}, \boldsymbol{\psi})$  further satisfies  $\|\mathbf{g}(t, \mathbf{z}, \boldsymbol{\psi})\| \leq b_1 \|\boldsymbol{\psi}\| \|\mathbf{z}\|$  and  $\boldsymbol{\psi}(t)$  converges to  $\mathbf{0}$  asymptotically as  $t \rightarrow \infty$ .

Finally, if  $\mathcal{Z} = \mathbb{R}^{n_z}$ , system (12) is globally exponentially/asymptotically stable. ■

*Lemma 2 (see [28, Lemma 1]):* The following system:

$$\dot{\mathbf{x}} = \begin{bmatrix} -k_1 & -k_2\phi(t) \\ k_4\phi(t) & 0 \end{bmatrix} \mathbf{x}, \quad \mathbf{x} \in \mathbb{R}^2 \quad (15)$$

is globally exponentially stable if  $k_1 > 0$ ,  $k_2k_4 > 0$ , and  $\phi(t)$  is persistently exciting. ■

*Lemma 3 (see [32, Theorem 1]):* Consider a directed graph  $\mathcal{G}$  satisfying Assumption 2. Define a matrix  $\mathcal{H}$  as in (3), two vectors as  $\mathbf{a} = \mathcal{H}^{-1}\mathbf{1}_N$  and  $\mathbf{b} = \mathcal{H}^{-T}\mathbf{1}_N$ , and two matrices as  $P = \text{diag}(b_i/a_i)$  and  $Q = P\mathcal{H} + \mathcal{H}^T P$ ,  $i \in \mathcal{V}$ . Then, both  $P$  and  $Q$  are positive definite. ■

### III. FORMATION CONTROL WITH UNKNOWN REFERENCE ORIENTATION

In this section, two dynamic control laws are proposed for the robots in groups  $\mathcal{V}_A$  and  $\mathcal{V}_B$ , respectively, so as to solve the formation tracking control problem with unknown reference orientation, i.e., Problem 1. Then, the global asymptotic stability of the resulting closed-loop system is established.

First, we obtain the following error dynamics by taking the time derivative of  $[x_{ei}, y_{ei}, s_{ei}, c_{ei}]^T$  defined in (7) and (8) along the trajectories of system (6):

$$\begin{aligned} \dot{x}_{ei} &= v_r - v_r c_{ei} - v_i + y_{ei}\omega_i \\ \dot{y}_{ei} &= v_r s_{ei} - x_{ei}\omega_i \\ \dot{s}_{ei} &= \omega_r - \omega_r c_{ei} - \omega_i + \omega_i c_{ei} \\ \dot{c}_{ei} &= \omega_r s_{ei} - s_{ei}\omega_i. \end{aligned} \quad (16)$$

To stabilize the above error dynamics, let us first consider the following controller:

$$\begin{aligned} v_i &= v_r + k_1 x_{ei} - k_2 \omega_r y_{ei} \\ \omega_i &= \omega_r + k_3 s_{ei}. \end{aligned} \quad (17)$$

Denote the error state by  $\boldsymbol{\chi}_i = [x_{ei}, y_{ei}, s_{ei}, c_{ei}]^T$ . Then, one can easily build the uniform exponential stability of the resulting closed-loop system consisting of (16) and (17) at  $\boldsymbol{\chi}_i = \mathbf{0}$  for all  $\boldsymbol{\chi}_i \in \mathcal{X}$ , where the domain  $\mathcal{X}$  is defined as

$$\mathcal{X} = \{(x, y, s, c) : x \in \mathbb{R}, y \in \mathbb{R}, s \in [-1, 1], c \in [0, 2]\} \quad (18)$$

which takes all error states into consideration except  $e_i^\theta = \pm k\pi$ , i.e.,  $c_{ei} = 1 - \cos e_i^\theta \neq 2$ . The above result is summarized as the following proposition, while its proof is given in Appendix B.

*Proposition 1:* Under Assumptions 1–3, for robot  $i \in \mathcal{V}_A$  with initial states satisfying  $\boldsymbol{\chi}_i(t_0) \in \mathcal{X}$ , the error state  $\boldsymbol{\chi}_i(t)$  of the system consisting of (16) and (17) exponentially converges to zero as  $t \rightarrow \infty$ . ■

However, in the design of controller (17), the reference orientation is assumed to be known so as to compute the error state  $s_{ei}$ . Next, we aim to design two adaptive control laws, based on

the result of Proposition 1, to stabilize the error dynamics (16) with no use of the reference orientation.

#### A. Control Law Design for Group A

For the follower  $i \in \mathcal{V}_A$ , the control law is designed as

$$\begin{aligned} v_i &= v_r + k_1 x_{ei} - k_2 \omega_r y_{ei} \\ \omega_i &= \omega_r + \gamma a v_r^2 (\hat{\zeta}_i + a v_r y_{ei}) \end{aligned} \quad (19)$$

with the observer

$$\dot{\hat{\zeta}}_i = -a v_r^2 \hat{\zeta}_i - a \dot{v}_r y_{ei} + a v_r \omega_i x_{ei} - a^2 v_r^3 y_{ei} \quad (20)$$

where the control gains satisfy  $k_1 > 0$ ,  $k_2 > 0$ ,  $0 < \gamma < 1/2$ ,  $a > 0$ , and the internal state  $\hat{\zeta}_i$  satisfies  $\hat{\zeta}_i(t_0) \neq a v_r(t_0) y_{ei}(t_0)$ . Note that  $\hat{\zeta}_i + a v_r y_{ei}$  is used to adaptively estimate the unknown orientation error  $s_{ei}$ .

The control law (19) depends on neither the reference orientation  $\theta_0$  nor the relative orientation measurement  $\theta_0 - \theta_i$ . To implement the control law, robots in group  $\mathcal{V}_A$  are supposed to be equipped with the onboard inertial measurement unit and LiDAR, so as to satisfy Assumption 3 and to obtain the error  $[x_{ei}, y_{ei}]^T$  by (7).

Now, we present the first main result of this article, stating that the control law consisting of (19) and (20) solves the tracking control problem for robots in group  $\mathcal{V}_A$  without using the reference orientation.

*Theorem 1:* If Assumptions 1–3 are satisfied, for follower  $i \in \mathcal{V}_A$  with any initial states  $[e_i^x(t_0), e_i^y(t_0), e_i^\theta(t_0)]^T \in \mathbb{R}^3$ , the control law consisting of (19) and (20) makes the tracking errors  $[x_{ei}(t), y_{ei}(t), s_{ei}(t), c_{ei}(t)]^T$  of system (16) globally asymptotically converge to zero as  $t \rightarrow \infty$ . ■

To analyze the stability of the resulting multirobot system consisting of group  $\mathcal{V}_A$ , we need to have the error system.

Denote the time-varying control gain as  $k_4 = \gamma a v_r^2$ , the relative orientation estimation as  $\tilde{s}_{ei} = \hat{\zeta}_i + a v_r y_{ei}$ , and the orientation estimation error as  $\tilde{s}_{ei} = \hat{\zeta}_i + a v_r y_{ei} - s_{ei}$ . Define the compact error state as  $\boldsymbol{\chi}_i = [x_{ei}, y_{ei}, s_{ei}, c_{ei}]^T$ , and  $\boldsymbol{\xi}_i = [\tilde{s}_{ei}, s_{ei}, c_{ei}]^T$  is viewed as an exogenous signal. Substituting (19) and (20) into (16), we obtain the following error system:

$$\begin{aligned} \dot{\boldsymbol{\chi}}_i &= F(t, \boldsymbol{\chi}_i) + G(t, \boldsymbol{\chi}_i, \boldsymbol{\xi}_i) \\ \dot{\boldsymbol{\xi}}_i &= H(t, \boldsymbol{\xi}_i) \end{aligned} \quad (21)$$

where

$$\begin{aligned} F(t, \boldsymbol{\chi}_i) &= \begin{bmatrix} -k_1 x_{ei} + (1 + k_2) \omega_r y_{ei} - v_r c_{ei} + k_4 y_{ei} s_{ei} \\ -\omega_r x_{ei} + v_r s_{ei} - k_4 s_{ei} x_{ei} \\ -k_4 s_{ei} + k_4 c_{ei} s_{ei} \\ -k_4 s_{ei}^2 \end{bmatrix} \\ H(t, \boldsymbol{\xi}_i) &= \begin{bmatrix} k_4 (1 - c_{ei}) s_{ei} + k_4 (1 - c_{ei}) \tilde{s}_{ei} - a v_r^2 \tilde{s}_{ei} \\ -k_4 s_{ei} + k_4 c_{ei} s_{ei} - k_4 \tilde{s}_{ei} + k_4 c_{ei} \tilde{s}_{ei} \\ -k_4 s_{ei}^2 - k_4 s_{ei} \tilde{s}_{ei} \end{bmatrix} \end{aligned}$$

$$G(t, \chi_i, \xi_i) = \begin{bmatrix} k_4 y_{ei} \tilde{s}_{ei} \\ -k_4 x_{ei} \tilde{s}_{ei} \\ -k_4 \tilde{s}_{ei} + k_4 c_{ei} \tilde{s}_{ei} \\ -k_4 s_{ei} \tilde{s}_{ei} \end{bmatrix}.$$

Now, the proof of Theorem 1 is stated as follows.

*Proof of Theorem 1:* Let us consider two cases of the initial orientations: (i)  $e_i^\theta(t_0) \in (-\pi + 2k\pi, \pi + 2k\pi)$  and (ii)  $e_i^\theta(t_0) = \pm k\pi$ , where  $k \in \mathbb{Z}$ .

*Case (i):* First, by Proposition 1, the nominal system  $\dot{\chi}_i = F(t, \chi_i)$  is uniformly exponentially stable at  $\chi_i = \mathbf{0}$  for all  $\chi_i \in \mathcal{X}$ . Second, we show the convergence of  $s_{ei}$ ,  $c_{ei}$ , and  $\tilde{s}_{ei}$ . Choose a Lyapunov function  $V_{(2)} = c_{ei} + \frac{1}{2} \tilde{s}_{ei}^2$ . Taking its time derivative along the trajectories of system (21) yields

$$\begin{aligned} \dot{V}_{(2)} &= -k_4 s_{ei}^2 - [av_r^2 - k_4(1 - c_{ei})] \tilde{s}_{ei}^2 - k_4 c_{ei} s_{ei} \tilde{s}_{ei} \\ &\leq -k_4 s_{ei}^2 - [av_r^2 - k_4|1 - c_{ei}|] \tilde{s}_{ei}^2 + k_4 |c_{ei}| |s_{ei}| |\tilde{s}_{ei}| \\ &\leq -k_4 s_{ei}^2 - (av_r^2 - k_4) \tilde{s}_{ei}^2 + 2k_4 |s_{ei}| |\tilde{s}_{ei}| \end{aligned} \quad (22)$$

where the last inequality holds since  $|1 - c_{ei}| \leq 1$  and  $|c_{ei}| < 2$ . Recall that  $k_4 = \gamma av_r^2$ , and then we have

$$\begin{aligned} \dot{V}_{(2)} &\leq -av_r^2 [\gamma s_{ei}^2 + (1 - \gamma) \tilde{s}_{ei}^2 + 2\gamma |s_{ei}| |\tilde{s}_{ei}|] \\ &\leq -av_r^2 [\gamma(|s_{ei}| - |\tilde{s}_{ei}|)^2 + (1 - 2\gamma) \tilde{s}_{ei}^2]. \end{aligned} \quad (23)$$

Since  $0 < \gamma < 1/2$ , we have  $\dot{V}_{(2)} \leq 0$ . Since  $\dot{V}_{(2)} = 0$  implies  $\tilde{s}_{ei} = 0$ , we have  $s_{ei} = 0$ . Since  $\chi_i \in \mathcal{X}$ ,  $s_{ei} = 0$  implies  $c_{ei} = 0$ . Then, it follows from the invariance principle [31, Theorem 4.4] that  $s_{ei}$ ,  $c_{ei}$ , and  $\tilde{s}_{ei}$  asymptotically converge to zero. Accordingly, the estimation state  $\hat{c}_i + av_r y_{ei}$  asymptotically converges to the orientation error  $s_{ei}$ , and equivalently, the exogenous signal  $\xi_i(t)$  converges to  $\mathbf{0}$  as  $t \rightarrow \infty$  asymptotically. Third, it holds that  $\|G_i(t, \chi_i, \xi_i)\| \leq 4k_4 \|\chi_i\| \|\xi_i\| + k_4 \|\xi_i\|$ . By Lemma 1(b), system (21) is uniformly asymptotically stable at  $\chi_i = \mathbf{0}$  for  $\chi_i \in \mathcal{X}$ .

*Case (ii):* Consider that if  $e_i^\theta = \pm k\pi$ , we have  $s_{ei} = 0$  and  $c_{ei} = 2$ , which reduces the orientation error system to

$$\dot{s}_{ei} = \gamma av_r^2 (\hat{c}_i + av_r y_{ei}), \quad \dot{c}_{ei} = 0.$$

Since we set  $\hat{c}_i(t_0) \neq av_r(t_0) y_{ei}(t_0)$ , it holds that  $\dot{s}_{ei}(t_0) \neq 0$ . Then, there will always be an instant  $t_1 > t_0$  such that  $e_i^\theta(t_1) \in (-\pi + 2k\pi, \pi + 2k\pi)$ , i.e.,  $\chi_i(t_1) \in \mathcal{X}$ . By the result of Case (i), we also have  $\chi_i(t) \rightarrow \mathbf{0}$  as  $t \rightarrow \infty$  given  $e_i^\theta(t_0) = \pm k\pi$ . The proof is thus completed. ■

As shown in the proof of Theorem 1, the tracking errors  $[x_{ei}, y_{ei}, s_{ei}, c_{ei}]^T$  and the orientation estimation error  $\tilde{s}_{ei} = \hat{c}_i + av_r y_{ei} - s_{ei}$  asymptotically converge to zero.

*Remark 3:* The design of the control law consisting of (19) and (20) is inspired by [28]. In [28], the resulting closed-loop system is proven to be uniformly exponentially stable under the assumption that the orientation error  $e_i^\theta = \theta_0 - \theta_i$  locates inside a closed and bounded interval  $e_i^\theta \in [-\theta_c, \theta_c]$ ,  $0 < \theta_c < \pi$ . In contrast, we build the global uniform exponential stability by setting an initial condition on the internal state, i.e.,  $\hat{c}_i(t_0) \neq av_r(t_0) y_{ei}(t_0)$ , which can be always satisfied, since both of  $v_r(t)$  and  $y_{ei}(t)$  are known to robots in group  $\mathcal{V}_A$ .

## B. Control Law Design for Group B

Since each follower in group  $\mathcal{V}_B$  has no knowledge of the leader's information directly, an online distributed observer is designed so as to estimate the position tracking error  $[e_i^x, e_i^y]^T$  and the reference orientation  $[s_0, c_0]^T$ . For each follower  $i$  in both groups  $\mathcal{V}_A \cup \mathcal{V}_B$ , we define the internal states  $[\hat{e}_i^x, \hat{e}_i^y, \hat{s}_i, \hat{c}_i]^T$ . By default, we assign  $[\hat{e}_i^x, \hat{e}_i^y, \hat{s}_i, \hat{c}_i]^T = [x_{ei} c_i - y_{ei} s_i, x_{ei} s_i + y_{ei} c_i, s_i, c_i]^T$  for follower  $i \in \mathcal{V}_A$ , as all followers are collaborative.

Then, the control law for follower  $i \in \mathcal{V}_B$  is designed as

$$\begin{aligned} v_i &= v_r + k_1 (\hat{e}_i^x c_i + \hat{e}_i^y s_i) - k_2 \omega_r (-\hat{e}_i^x s_i + \hat{e}_i^y c_i), \\ \omega_i &= \omega_r + k_3 (\hat{s}_i c_i - \hat{c}_i s_i) \end{aligned} \quad (24)$$

with the observer

$$\begin{aligned} \dot{\hat{e}}_i^x &= v_r \hat{c}_i - v_i c_i + \sum_{j \in \mathcal{N}_i} a_{ij} ((\hat{e}_j^x - \hat{e}_i^x) + (x_j - x_i) + d_{ij}^x) \\ \dot{\hat{e}}_i^y &= v_r \hat{s}_i - v_i s_i + \sum_{j \in \mathcal{N}_i} a_{ij} ((\hat{e}_j^y - \hat{e}_i^y) + (y_j - y_i) + d_{ij}^y) \\ \dot{\hat{s}}_i &= \omega_r \hat{c}_i + \sum_{j \in \mathcal{N}_i} a_{ij} (\hat{s}_j - \hat{s}_i) \\ \dot{\hat{c}}_i &= -\omega_r \hat{s}_i + \sum_{j \in \mathcal{N}_i} a_{ij} (\hat{c}_j - \hat{c}_i) \end{aligned} \quad (25)$$

where  $k_3$  is a positive control gain, and the internal states  $\hat{s}_i$  and  $\hat{c}_i$  satisfy  $\hat{s}_i(t_0) c_i(t_0) + \hat{c}_i(t_0) s_i(t_0) \neq 0$ .

Note that  $[\hat{e}_i^x, \hat{e}_i^y]^T$  is used to estimate the position error  $[e_i^x, e_i^y]^T$ , and  $[\hat{s}_i, \hat{c}_i]^T$  is used to estimate the reference orientation  $[s_0, c_0]^T$ .

The followers in group  $\mathcal{V}_B$  are also supposed to possess with the same sensors with those in  $\mathcal{V}_A$ . Thus, the relative positions of robot  $i$ 's neighbors,  $\mathbf{p}_j - \mathbf{p}_i$ , and its own orientation variables  $s_i$  and  $c_i$  are measured, as stated in Assumption 3. The estimated states of its neighbors,  $\hat{e}_j^x$ ,  $\hat{e}_j^y$ ,  $\hat{s}_j$ , and  $\hat{c}_j$ , are transmitted via the inter-robot communication. Since all of the required measurements and communications are local, control law (24) can be implemented in a fully distributed manner.

Now, the second result of this article is given as follows.

*Theorem 2:* If Assumptions 1–3 are satisfied, for follower  $i \in \mathcal{V}_B$  with any initial states  $[e_i^x(t_0), e_i^y(t_0), e_i^\theta(t_0)]^T \in \mathbb{R}^3$ , the control law consisting of (24) and (25) for follower  $i \in \mathcal{V}_B$  makes the tracking errors  $[x_{ei}(t), y_{ei}(t), s_{ei}(t), c_{ei}(t)]^T$  of system (16) asymptotically converge to zero as  $t \rightarrow \infty$ . ■

To analyze the stability of the resulting multirobot system consisting of group  $\mathcal{V}_B$ , we need to have the error system.

Define the estimation error as  $\zeta_i = [\tilde{x}_i, \tilde{y}_i, \tilde{s}_i, \tilde{c}_i]^T$  with

$$\tilde{x}_i = \hat{e}_i^x - e_i^x, \quad \tilde{y}_i = \hat{e}_i^y - e_i^y, \quad \tilde{s}_i = \hat{s}_i - s_0, \quad \tilde{c}_i = \hat{c}_i - c_0 \quad (26)$$

and the estimation error after coordinate transformation as

$$\tilde{x}_{ei} = \hat{e}_i^x c_i + \hat{e}_i^y s_i - x_{ei}, \quad \tilde{y}_{ei} = -\hat{e}_i^x s_i + \hat{e}_i^y c_i - y_{ei}. \quad (27)$$

Substituting (24), (26), and (27) into (16) yields the following error system:

$$\begin{aligned}\dot{\chi}_i &= F(t, \chi_i) + \bar{G}(t, \chi_i, \zeta_i) \\ \dot{\zeta}_i &= \bar{H}(t, \zeta_i)\end{aligned}\quad (28)$$

where  $\chi_i$  and  $F(t, \chi_i)$  are defined in (21), and  $\bar{G}(t, \chi_i, \zeta_i)$  and  $\bar{H}(t, \zeta_i)$  are defined as

$$\begin{aligned}\bar{G}(t, \chi_i, \zeta_i) &= \begin{bmatrix} -k_1 \tilde{x}_{ei} + k_2 \omega_r \tilde{y}_{ei} + k_3 y_{ei} c_i \tilde{s}_i - k_3 y_{ei} s_i \tilde{c}_i \\ -k_3 x_{ei} c_i \tilde{s}_i + k_3 x_{ei} s_i \tilde{c}_i \\ -k_3 c_i \tilde{s}_i + k_3 s_i \tilde{c}_i + k_3 c_{ei} c_i \tilde{s}_i - k_3 c_{ei} s_i \tilde{c}_i \\ -k_3 s_{ei} c_i \tilde{s}_i + k_3 s_{ei} s_i \tilde{c}_i \end{bmatrix} \\ \bar{H}(t, \zeta_i) &= \begin{bmatrix} \sum_{j \in \mathcal{N}_i} a_{ij} (\tilde{x}_j - \tilde{x}_i) + v_r \tilde{c}_i \\ \sum_{j \in \mathcal{N}_i} a_{ij} (\tilde{y}_j - \tilde{y}_i) + v_r \tilde{s}_i \\ \omega_r \tilde{c}_i + \sum_{j \in \mathcal{N}_i} a_{ij} (\tilde{s}_j - \tilde{s}_i) \\ -\omega_r \tilde{s}_i + \sum_{j \in \mathcal{N}_i} a_{ij} (\tilde{c}_j - \tilde{c}_i) \end{bmatrix}.\end{aligned}$$

To prove Theorem 2, we first show the convergence of the distributed observer (25), i.e., the stability of estimation error system  $\dot{\zeta}_i = \bar{H}(t, \zeta_i)$ , which is stated in the following proposition. The detailed proof is given in Appendix C.

**Proposition 2:** Under Assumptions 1–3, for each follower  $i \in \mathcal{V}_B$  with any initial states  $[\hat{e}_i^x(t_0), \hat{e}_i^y(t_0), \hat{s}_i(t_0), \hat{c}_i(t_0)]^T$ , observer (25) makes  $[\hat{e}_i^x(t), \hat{e}_i^y(t), \hat{s}_i(t), \hat{c}_i(t)]^T$  asymptotically converge to  $[e_i^x(t), e_i^y(t), s_0(t), c_0(t)]^T$  as  $t \rightarrow \infty$ , i.e., the estimation error  $\zeta_i(t) = [\tilde{x}_i(t), \tilde{y}_i(t), \tilde{s}_i(t), \tilde{c}_i(t)]^T$  asymptotically converges to  $\mathbf{0}$  as  $t \rightarrow \infty$ . ■

Now, we present the proof of Theorem 2.

**Proof of Theorem 2:** We still consider two cases of the initial orientations: (i)  $e_i^\theta(t_0) \in (-\pi + 2k\pi, \pi + 2k\pi)$  and (ii)  $e_i^\theta(t_0) = \pm k\pi$ , where  $k \in \mathbb{Z}$ .

*Case (i):* By (26) and (27), we have

$$\begin{bmatrix} \tilde{x}_{ei} \\ \tilde{y}_{ei} \end{bmatrix} = \begin{bmatrix} c_i & s_i \\ -s_i & c_i \end{bmatrix} \begin{bmatrix} \tilde{x}_i \\ \tilde{y}_i \end{bmatrix}.\quad (29)$$

Then, we have  $\|[\tilde{x}_{ei}, \tilde{y}_{ei}]^T\| = \|[\tilde{x}_i, \tilde{y}_i]^T\|$ . It follows that  $\max(|\tilde{x}_{ei}|, |\tilde{y}_{ei}|) \leq \|[\tilde{x}_{ei}, \tilde{y}_{ei}]^T\| = \|[\tilde{x}_i, \tilde{y}_i]^T\| \leq \|\zeta_i\|$ .

Accordingly, we have  $\|\bar{G}(t, \chi_i, \zeta_i)\| \leq 8k_3 \|\chi_i\| \|\zeta_i\| + (k_1 + k_2 b_\omega + 2k_3) \|\zeta_i\|$ . By Proposition 1, the nominal system  $\dot{\chi}_i = F(t, \chi_i)$  is uniformly exponentially stable for all  $\chi_i \in \mathcal{X}$ . By Proposition 2, the exogenous signal  $\zeta_i(t) \rightarrow \mathbf{0}$  asymptotically as  $t \rightarrow \infty$ . Therefore, by Lemma 1(b), system (28) is also uniformly asymptotically stable at  $\chi_i = \mathbf{0}$  for all  $\chi_i \in \mathcal{X}$ .

*Case (ii):* Considering that  $e_i^\theta = \pm k\pi$ , we have  $s_{ei} = 0$  and  $c_{ei} = 2$ , which reduces the orientation error system to

$$\dot{s}_{ei} = k_3 (\hat{s}_i c_i - \hat{c}_i s_i), \quad \dot{c}_{ei} = 0.$$

By a similar analysis as the proof of Theorem 1, we also have  $\chi_i(t) \rightarrow \mathbf{0}$  as  $t \rightarrow \infty$  given  $e_i^\theta(t_0) = \pm k\pi$ . The proof is, thus, completed. ■

## IV. EXPERIMENT

In this section, we present the experimental results to illustrate the effectiveness of the proposed control approach.

---

**Algorithm 1:** Distributed Formation Control of Mobile Robots With Unknown Reference Orientation (for Robot  $i \in \mathcal{V}$ ).

---

**Initiation:** Neighbors  $\mathcal{N}_i$ ; Desired Relative Positions  $d_{ij}, j \in \mathcal{N}_i$ ; Reference Driving Velocity  $v_r$ ; Reference Steering Velocity  $\omega_r$ .

**Input:** Neighbors' Relative Position  $p_j(t) - p_i(t), j \in \mathcal{N}_i$  by Sensing; Neighbors' Internal States  $[\hat{e}_j^x(t), \hat{e}_j^y(t), \hat{s}_j(t), \hat{c}_j(t)]^T$  for  $i \in \mathcal{V}_B$  by Communication;

**Output:** Trajectory  $[x_i(t), y_i(t), \theta_i(t)]^T, t \geq t_0$ ;

**while** not converge **do**

**if**  $Q_i = \emptyset$  **then**

**if**  $i \in \mathcal{V}_A$  **then**

      Implements (19) and (20) on (1);

**else**  $\{i \in \mathcal{V}_B\}$

      Implements (24) and (25) on (1);

**end if**

**else**  $\{Q_i \neq \emptyset\}$

    Implements (30) on (1);

**end if**

**end while**

---

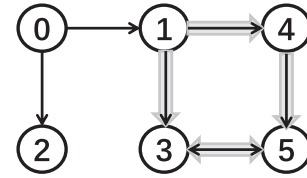


Fig. 3. Directed graph  $\mathcal{G}$  among the multirobot system. Thin edges: sensing. Thick edges: sensing and communication.

### A. Setup

Laboratorial experiment is conducted on six TurtleBot3 Burger mobile robots. They are equipped with individual computer boards powered by Ubuntu Mate and Robotic Operating System (ROS). The motion of each robot is driven by the driving and steering velocity commands from the onboard ROS, and its kinematics are thus described by the nonholonomic model (1). Owing to the limited sensing capability of TurtleBot3 Burger mobile robots, we use the VICON indoor positioning system (VICON Motion Systems, OMG PLC Company), instead of real onboard sensors, to localize the mobile robots and record their motion, which is the same setting as that in [33]. The VICON motion tracking system was equipped with ten VICON Bonita cameras to track each robot fixed with five reflective pearl markers for identification. Based on this setting, the relative positions of neighboring robots, required for the control laws consisting of (19), (20), (24), and (25), are computed and transmitted to each robot by the VICON system. Since the driving and steering velocity control inputs are computed and implemented by each robot itself, rather than a centralized master computer, this VICON-based multirobot platform, which is the same as the settings in [33] and [34], is capable enough to examine the effectiveness of the proposed distributed control approach in the

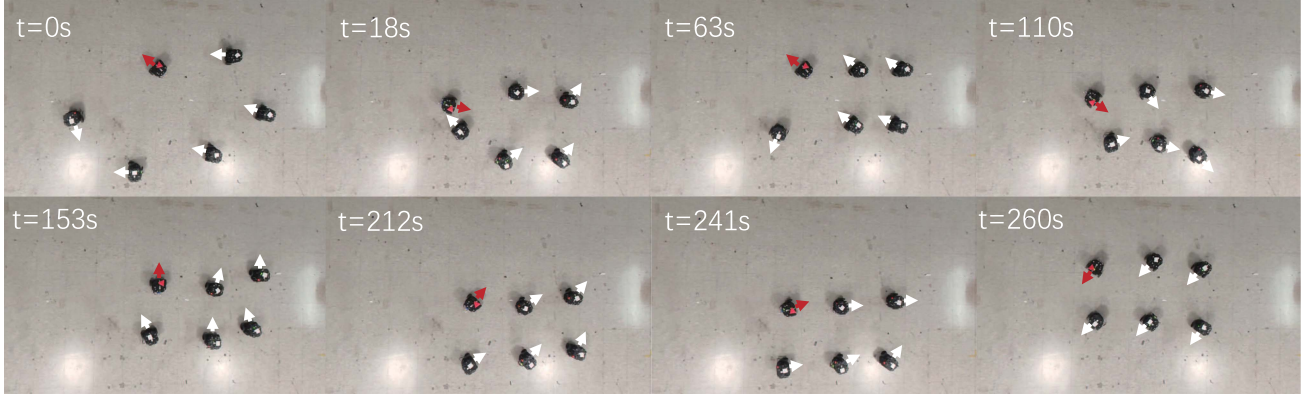


Fig. 4. Snapshots of the on-site multirobot system in the experiment.

presence of many practical issues, such as motor offset, wear and tear of wheels, delays, and some external perturbations, such as noise and friction.

### B. Collision Avoidance

To handle the collision avoidance, we adopt a behavior-based switching algorithm. As in [33], robots are assumed to be with the capability of proximity perception, which can be physically realized by short-range infrared proximity sensors. For convenience, in the experiment, the VICON indoor positioning system is utilized to do proximity perception for each robot instead of onboard sensors. We set a proximity threshold  $d_s > 0$  to determine a proximity-based neighboring set as  $Q_i = \{j : \|\mathbf{p}_j - \mathbf{p}_i\| \leq d_s\}$ . For robot  $i$ , the switching algorithm for the actual driving and steering velocity  $[\bar{v}_i, \bar{\omega}_i]^T$  is designed as

$$[\bar{v}_i, \bar{\omega}_i]^T = \begin{cases} [v_i, \omega_i]^T - [\delta_{vi}, \delta_{\omega i}]^T, & \text{if } Q_i \neq \emptyset \\ [v_i, \omega_i]^T, & \text{otherwise} \end{cases} \quad (30)$$

where

$$\begin{bmatrix} \delta_{vi} \\ \delta_{\omega i} \end{bmatrix} = \begin{bmatrix} c_i & s_i \\ -s_i & c_i \end{bmatrix} \sum_{j \in Q_i} \frac{1}{\|\mathbf{p}_j - \mathbf{p}_i\|^2} (\mathbf{p}_j - \mathbf{p}_i).$$

Note that the offsets  $\delta_{vi}$  and  $\delta_{\omega i}$  impel robots to move away from each other. More importantly, they are faster as the distance becomes smaller. This method is effective since the control laws presented in Section III make the multirobot system globally uniformly asymptotically stable, which implies that the convergence to the desired formation is independent of the initial instants or states. To this end, this switching algorithm would not influence the convergence of the multirobot system to the final desired formation, as the switching algorithm can be viewed as tuning the initial instants or states.

### C. Results

The multirobot system consists of one physical leader (labeled 0) and five followers (labeled 1–5) with kinematics (1). Owing to the limited workspace, we set the leader's trajectory

as a circle with the reference driving and steering velocities as  $v_r = 0.05$  m/s and  $\omega_r = 0.2$  rad/s, which also satisfies Assumption 1. The desired rectangle formation is determined by the leader's position  $\mathbf{p}_0(t)$  and the following relative positions:  $\mathbf{d}_{10} = [0.6 \text{ m}, 0]^T$ ,  $\mathbf{d}_{20} = [0, -0.6 \text{ m}]^T$ ,  $\mathbf{d}_{30} = [1.2 \text{ m}, 0]^T$ ,  $\mathbf{d}_{40} = [0.6 \text{ m}, -0.6 \text{ m}]^T$ ,  $\mathbf{d}_{50} = [1.2 \text{ m}, -0.6 \text{ m}]^T$ . The directed graph is given in Fig. 3. To facilitate the understanding of the proposed control approach in the experiment, we summarize it as Algorithm 1.

The followers are also divided into two groups  $\mathcal{V}_A = \{1, 2\}$  and  $\mathcal{V}_B = \{3, 4, 5\}$ . Set control gains  $k_1 = 0.2$ ,  $k_2 = 0.2$ ,  $k_3 = 0.4$ ,  $a = 30$ ,  $\gamma = 0.3$ , and  $a_{ij} = 1$ , for  $i \in \mathcal{V}_B$  and  $j \in \mathcal{N}_i$ . The initial estimates  $[\hat{s}_i(t_0), \hat{e}_i^x(t_0), \hat{e}_i^y(t_0), \hat{s}_i(t_0), \hat{c}_i(t_0)]^T$  are set randomly. Set the initial positions and orientations of six robots randomly. Moreover, based on the size of TurtleBot3 robots, the proximity threshold is set as  $d_s = 0.23$  m. Then, the control law consisting of (19), (20), (24), and (25) together with the collision avoidance algorithm (30) are implemented on the multirobot platform.

As illustrated in Fig. 4, five controlled follower robots aim to track the leader's motion and form a rectangle formation with the leader in practical workspace. The trajectories during formation evolvment are given in Fig. 5. As shown in Figs. 6 and 7, all tracking errors  $[x_{ei}, y_{ei}, s_{ei}, c_{ei}]^T$  and all estimates  $[\hat{s}_i, \hat{e}_i^x, \hat{e}_i^y, \hat{s}_i, \hat{c}_i]^T$  are convergent. Note that the tracking error of follower 2, labeled by the yellow line in Fig. 6, converges to zero more slowly than that of the other four followers, due to the fact that we set the initial orientation error of follower 2 much larger than the other followers. Besides, the change of relative distances  $r_{ij}$ ,  $j \in \mathcal{V}$ , is given in Fig. 8. It is shown that the distance between robot 0 and robot 2 turns equal to the proximity threshold  $d_s$  at  $t = 23$  s. The driving and steering velocity control inputs are thus switched to (30), and the collision avoidance mechanism takes effect. Consequently, no collision occurs during the formation evolvment.

During this experiment, the six robots are often misidentified by the VICON system since there exist too many reflective pearl markers, which brings about much noise and inaccuracy to the localization and the relative position measurements. Moreover, it is rather difficult for the real robots to realize a perfect servoing

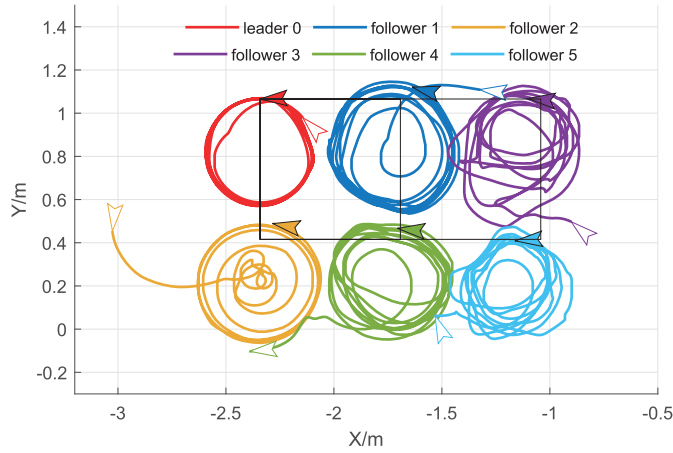


Fig. 5. Trajectories of mobile robots in the experiment.

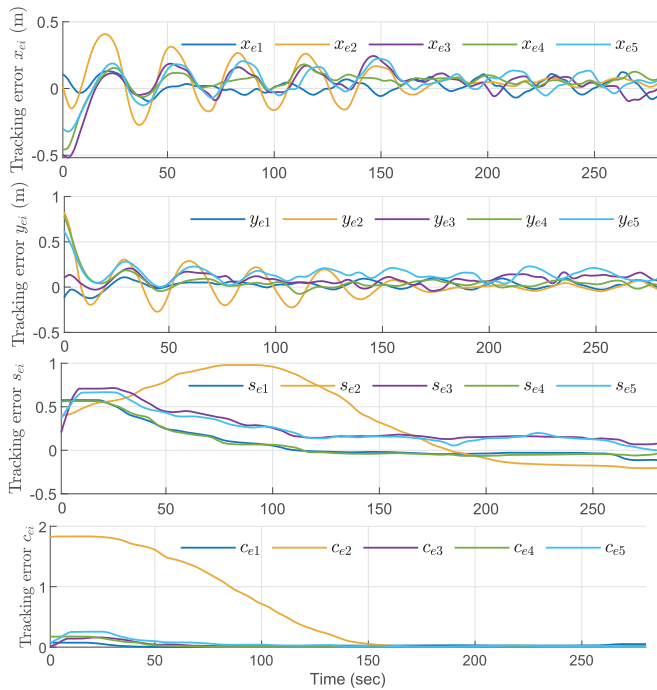


Fig. 6. Tracking errors of each follower in the experiment.

control of the designed driving and steering velocities. Owing to the existence of these inaccuracy and noise, it is not practical for the errors to converge to zero. The desired formation is considered to be achieved when the absolute values of the tracking errors  $x_{ei}$  and  $y_{ei}$  are less than 0.2 m. Therefore, although the filtering had some effect on the convergence speed, the multirobot system finally converges to the desired rectangle formation. A video recording this experiment is provided in the supplementary material (see also in [https://youtu.be/5N\\_pg1ia9wQ](https://youtu.be/5N_pg1ia9wQ)) to further demonstrate the effectiveness of our proposed control approach.

*Remark 4:* In the experiment, the trajectories of the followers are not that smooth, since the noises and inaccuracy brought by the VICON indoor positioning system cannot be avoided. The

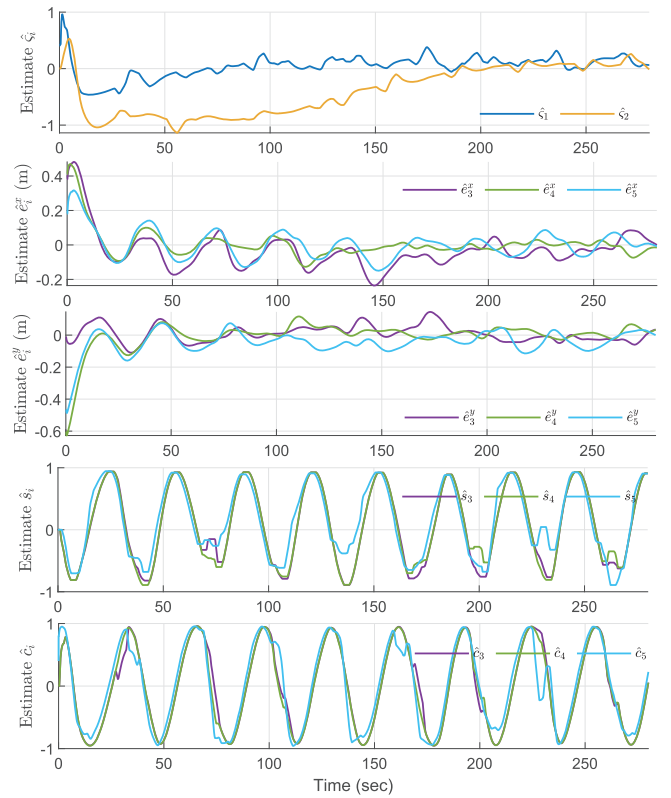


Fig. 7. Estimates of each follower in the experiment.

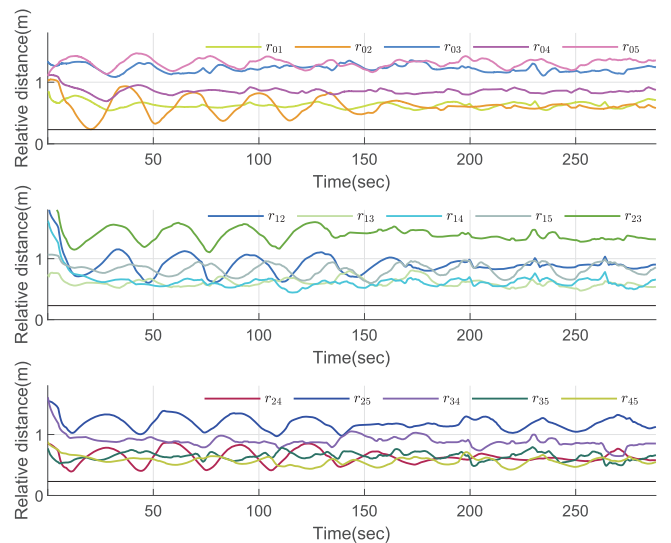


Fig. 8. Relative distances  $r_{ij}$ ,  $\forall i \in \mathcal{V}, j \in \mathcal{V}$  in the experiment. Black horizontal line: the proximity threshold  $d_s$ .

existence of too many reflective pearl markers brings about some inevitable localization inaccuracy of the VICON system. Despite some nonsmoothness curves, the convergence of the multirobot system is still clear in the experiment, which shows that the laboratorial experiment illustrates the fundamental effectiveness of our control approach.

*Remark 5:* In the experiment, we adopt a behavior-based switching algorithm to avoid inter-robot collisions, and it yields

a fairly good performance. Theoretically, it may also bring possible deadlocks when multirobot systems scale largely. In fact, the developed control law could be well incorporated with many collision avoidance approaches, either the behavior-based switching algorithm that we have used or the control barrier function (CBF) approach [35]. For the latter one, the proposed control law could be used as the nominal controller in the CBF approach. In this article, we do not employ the CBF approach, since it would require high computational load in online solving the quadratic programming problem.

## V. CONCLUSION

In this article, a distributed control approach was proposed for networked nonholonomic mobile robots to solve the leader-following formation tracking problem with unknown reference orientation. The network topology among the mobile robots was described by a directed graph containing a directed spanning tree. Particularly, the proposed control approach does not require the information of reference orientation or any relative orientation measurements among the neighboring robots. Moreover, the experiment conducted on TurtleBot3 Burger mobile robots is presented to show the effectiveness of our proposed control approach. There are some directions for the future work. First, we hope to equip the TurtleBot3 Burger robots with onboard sensors like LiDAR as well as more effective filtering algorithms to build a sensor-based platform for fully decentralized control of multirobot systems. Second, we aim to extend the result to the formation control of 3-D robots on  $SO(3)$  in absence of reference orientation. Finally, formation control problems of multirobot systems with time-varying/switching network and the conditions for connectivity preservation will be further investigated.

## APPENDIX A PROOF OF LEMMA 1

Since the nominal system (13) is uniformly exponentially stable at  $z = 0$  for  $z \in \mathcal{Z}$ , by the converse Lyapunov theorem [31, Theorem 4.14], there exists a function  $V : [0, \infty) \times \mathcal{Z} \rightarrow \mathbb{R}$  which satisfies: 1)  $b_3 \|z\|^2 \leq V(t, z) \leq b_4 \|z\|^2$ ; 2)  $\frac{\partial V}{\partial t} + \frac{\partial V}{\partial z} \mathbf{f}(t, z) \leq -b_5 \|z\|^2$ ; and 3)  $\|\frac{\partial V}{\partial z}\| \leq b_6 \|z\|$ , for some positive constants  $b_3, b_4, b_5$ , and  $b_6$ . Then, the time derivative of  $V$  along the trajectories of system (12) satisfies

$$\dot{V} \leq -b_5 \|z\|^2 + b_1 b_6 \|z\|^2 \|\psi\| + b_2 b_6 \|z\| \|\psi\|. \quad (31)$$

To prove Lemma 1(a), define  $W = \sqrt{V}$ , and we have  $\dot{W} = \dot{V}/2\sqrt{V}$ . It follows from (31) that  $\dot{W} \leq -\frac{1}{2}(\frac{b_5}{b_4} - \frac{b_1 b_6}{b_3} \|\psi\|)W + \frac{b_2 b_6}{2\sqrt{b_3}} \|\psi\|$ . By the comparison lemma [31, Lemma 3.4] and  $W \geq \sqrt{b_3} \|z(t)\|$ , we have

$$\|z(t)\| \leq \sqrt{\frac{b_4}{b_3}} \phi(t, t_0) \|z(t_0)\| + \frac{b_2 b_6}{2b_3} \int_{t_0}^t \phi(t, \tau) \|\psi(\tau)\| d\tau \quad (32)$$

with the transition function

$$\phi(t, t_0) = \exp \left[ -\frac{b_5}{2b_4} (t - t_0) + \frac{b_1 b_6}{2b_3} \int_{t_0}^t \|\psi(\tau)\| d\tau \right]. \quad (33)$$

When  $\psi(t)$  converges to  $\mathbf{0}$  exponentially as  $t \rightarrow \infty$ , then the trajectory satisfies  $\|\psi(t)\| \leq b_7 \|\psi(t_0)\| e^{-\beta(t-t_0)}$  with some positive constants  $b_7$  and  $\beta$ . Then, there exist two constants  $0 < \epsilon < b_3 b_5 / b_1 b_4 b_6$  and  $\vartheta > b_7 \|\psi(t_0)\| / \beta$  such that  $\psi(t)$  satisfies  $\int_{t_0}^t \|\psi(\tau)\| d\tau \leq b_7 \|\psi(t_0)\| \int_{t_0}^t e^{-\beta(\tau-t_0)} d\tau = \frac{b_7}{\beta} \|\psi(t_0)\| (1 - e^{-\beta(t-t_0)}) \leq \epsilon(t - t_0) + \vartheta$ . Choose two constants  $\alpha$  and  $b_8$  such that  $\alpha = \frac{1}{2}(\frac{b_5}{b_4} - \epsilon \frac{b_1 b_6}{b_3}) > 0$ ,  $\alpha \neq \beta$ , and  $b_8 = \exp(\frac{b_1 b_6 \vartheta}{2b_3}) \geq 1$ .

It follows from (32) that  $\|z(t)\| \leq \sqrt{\frac{b_4}{b_3}} b_8 \|z(t_0)\| e^{-\alpha(t-t_0)} + \frac{b_2 b_6 b_7 b_8}{2b_3} \|\psi(t_0)\| \int_{t_0}^t e^{-\alpha(t-\tau)} e^{-\beta(\tau-t_0)} d\tau$ .

Note that  $\int_{t_0}^t e^{-\alpha(t-\tau)} e^{-\beta(\tau-t_0)} d\tau = \frac{e^{-\alpha(t-t_0)} - e^{-\beta(t-t_0)}}{\beta - \alpha} \leq (\beta - \alpha)^{-1} e^{-\alpha(t-t_0)}$  holds, since  $\alpha \neq \beta$ . Thus, we have  $\|z(t)\| \leq \kappa \|z(t_0)\| e^{-\alpha(t-t_0)}$  with the constant  $\kappa = \sqrt{\frac{b_4}{b_3}} b_8 + \frac{b_2 b_6 b_7 b_8}{2b_3(\beta - \alpha)} \|\psi(t_0)\| / \|z(t_0)\|$ . Therefore, system (12) is uniformly exponentially stable at  $z = 0$  for  $z \in \mathcal{Z}$  if  $\psi(t)$  converges to  $\mathbf{0}$  exponentially as  $t \rightarrow \infty$ .

To prove Lemma 1(b), where  $\psi(t)$  converges to  $\mathbf{0}$  asymptotically as  $t \rightarrow \infty$ , we use the fact that given any  $\epsilon_1$ , there exists  $T_1(\epsilon_1) > 0$  such that  $\|\psi(t)\| \leq \epsilon_1$ ,  $t \geq T_1(\epsilon_1)$ . Choose  $\epsilon_1 < b_5 / b_1 b_6$ , and (31) becomes

$$\dot{V} \leq -(b_5 - b_1 b_6 \epsilon_1)(1 - \epsilon_2) \|z\|^2 \quad (34)$$

for all  $t \geq T_1(\epsilon_1)$  and  $\|z\| \geq b_2 b_6 \epsilon_1 / \epsilon_2 (b_5 - b_1 b_6 \epsilon_1)$ , and  $0 < \epsilon_2 < 1$ . By [31, Theorem 4.18], we have  $\|z(t)\| \leq \varphi(\|z(t_0)\|, t - t_0) + \sqrt{\frac{b_4}{b_3} \frac{b_1 b_6 \epsilon_1}{\epsilon_2 (b_5 - b_1 b_6 \epsilon_1)}}$ , where  $\varphi$  is a class  $\mathcal{KL}$  function. Since  $\varphi(\|z(t_0)\|, t - t_0)$  converges to 0 as  $t \rightarrow \infty$ , given any  $\epsilon_3$ , there exists  $T_2(\epsilon_3)$  such that  $\varphi(\|z(t_0)\|, t - t_0) \leq \frac{\epsilon_3}{2}$ ,  $t \geq T_2(\epsilon_3)$ . Choose  $\epsilon_1$  and  $\epsilon_2$  such that  $\sqrt{\frac{b_4}{b_3} \frac{b_1 b_6 \epsilon_1}{\epsilon_2 (b_5 - b_1 b_6 \epsilon_1)}} \leq \frac{\epsilon_3}{2}$ . Thus, we have  $\|z(t)\| \leq \epsilon_3$ ,  $t \geq T_3$  with  $T_3(\epsilon_3) = \max(T_1(\epsilon_1(\epsilon_3)), T_2(\epsilon_3))$ , which shows that  $z(t)$  converges to  $\mathbf{0}$  as  $t \rightarrow \infty$ . Therefore, system (12) is uniformly asymptotically stable at  $z = 0$  for  $z \in \mathcal{Z}$  if  $\psi(t)$  converges to  $\mathbf{0}$  asymptotically as  $t \rightarrow \infty$ .

To prove Lemma 1(c), where  $\|g(t, z, \psi)\| \leq b_1 \|\psi\| \|z\|$ , substitute  $b_2 = 0$  into (34) and we have  $\dot{V} \leq -(b_5 - b_1 b_6 \epsilon_1) \|z\|^2$  for all  $t \geq T_1(\epsilon_1)$  with  $\epsilon_1 < b_5 / b_1 b_6$ . By [31, Theorem 4.10], system (12) is uniformly exponentially stable at  $z = 0$  for  $z \in \mathcal{Z}$ .

Finally, if  $\mathcal{Z} = \mathbb{R}^{n_z}$ , Lemma 1 holds for all initial states, showing that system (12) is global exponentially/asymptotically stable.  $\blacksquare$

## APPENDIX B PROOF OF PROPOSITION 1

Denote  $z_{1i} = [x_{ei}, y_{ei}]^T$ ,  $z_{2i} = [s_{ei}, c_{ei}]^T$ . Then, the closed-loop system consisting of (16) and (17) can be written as

$$\begin{aligned} \dot{z}_{1i} &= \mathbf{f}(t, z_{1i}) + \mathbf{g}(t, z_{1i}, z_{2i}) \\ \dot{z}_{2i} &= \mathbf{h}(t, z_{2i}) \end{aligned} \quad (35)$$

where

$$\mathbf{f} = \begin{bmatrix} -k_1 & (1 + k_2)\omega_r \\ -\omega_r & 0 \end{bmatrix}, \quad \mathbf{h} = \begin{bmatrix} -k_3 s_{ei} + k_3 c_{ei} s_{ei} \\ -k_3 s_{ei}^2 \end{bmatrix} \quad (36)$$

and  $\mathbf{g} = [-v_r c_{ei} + k_3 y_{ei} s_{ei}, v_r s_{ei} - k_3 x_{ei} s_{ei}]^T$ .

First, since  $\omega_r$  is persistently exciting under Assumption 1, it follows from Lemma 2 that system  $\dot{z}_{1i} = \mathbf{f}(t, z_{1i})$  is uniformly exponentially stable for  $[z_{1i}, z_{2i}]^T \in \mathcal{X}$ . Next, we show that system  $\dot{z}_{2i} = \mathbf{h}(t, z_{2i})$  is also uniformly exponentially stable for  $[z_{1i}, z_{2i}]^T \in \mathcal{X}$ . Choose a Lyapunov function candidate  $V_{(1)} = c_{ei}$ , since  $c_{ei} \geq 0$ . Taking its derivative along the trajectories of system  $\dot{z}_{2i} = \mathbf{h}(t, z_{2i})$  yields  $\dot{V}_{(1)} \leq -k_4 s_{ei}^2 \leq 0$ . For  $[z_{1i}, z_{2i}]^T \in \mathcal{X}$ , we have  $-1 \leq s_{ei} \leq 1$  and  $0 \leq c_{ei} < 2$ . Accordingly,  $s_{ei} = 0$  implies  $c_{ei} = 0$ . By the invariance principle [31, Theorem 4.4], we have  $c_{ei} \rightarrow 0$ . Then, consider the system  $\dot{s}_{ei} = -k_3 s_{ei} + k_3 c_{ei} s_{ei}$  as a nominal system  $\dot{s}_{ei} = -k_3 s_{ei}$  with a perturbation  $k_3 c_{ei} s_{ei}$ . It is obvious that the nominal system  $\dot{s}_{ei} = -k_3 s_{ei}$  is uniformly exponentially stable. Moreover, the perturbation  $k_3 c_{ei} s_{ei}$  satisfies  $|k_3 c_{ei} s_{ei}| \leq k_3 |c_{ei}| |s_{ei}|$  and  $c_{ei} \rightarrow 0$ . By Lemma 1(c), system  $\dot{s}_{ei} = -k_3 s_{ei} + k_3 c_{ei} s_{ei}$  is uniformly exponentially stable. As a result, both  $s_{ei}(t)$  and  $c_{ei}(t)$  converge to 0 exponentially as  $t \rightarrow \infty$ , that is, system  $\dot{z}_{2i} = \mathbf{h}(t, z_{2i})$  is uniformly exponentially stable for  $[z_{1i}, z_{2i}]^T \in \mathcal{X}$ . Under Assumption 1, there exists a positive constant  $b_v$  such that  $|v_r| \leq b_v$ . Besides, we have  $\max(|x_{ei}|, |y_{ei}|) \leq \|z_{1i}\|$ , and  $\max(|s_{ei}|, |c_{ei}|) \leq \|z_{2i}\|$ . Then,  $\mathbf{g}(t, z_{1i}, z_{2i})$  satisfies  $\|\mathbf{g}(t, z_{1i}, z_{2i})\| \leq 2k_3 \|z_{1i}\| \|z_{2i}\| + 2b_v \|z_{2i}\|$ . Therefore, by Lemma 1(a), system (35), i.e.,  $\dot{\chi}_i = F(t, \chi_i)$ , is uniformly exponentially stable for  $\chi_i \in \mathcal{X}$ . The proof is completed. ■

### APPENDIX C PROOF OF PROPOSITION 2

First, we show the convergence of  $\tilde{s}_i$  and  $\tilde{c}_i$  for  $i \in \mathcal{V}_A \cup \mathcal{V}_B$ . For the follower  $i \in \mathcal{V}_A$ , since  $\hat{s}_i = s_i$ , taking the time derivative of  $\tilde{s}_i = \hat{s}_i - s_0$  along trajectories of system (6) yields

$$\dot{\tilde{s}}_i = \dot{\hat{s}}_i - \dot{s}_0 = \omega_r \tilde{c}_i + c_i(t) \tilde{\omega}_i(t) \quad (37)$$

where  $\tilde{\omega}_i(t) = \omega_i(t) - \omega_r(t)$ . Similarly, we have

$$\begin{aligned} \dot{\tilde{s}}_i &= \omega_r \tilde{c}_i - \tilde{s}_i + \mu_i(t) \\ \dot{\tilde{c}}_i &= -\omega_r \tilde{s}_i - \tilde{c}_i + \nu_i(t), \quad i \in \mathcal{V}_A \end{aligned} \quad (38)$$

where we define  $\mu_i(t) = c_i(t) \tilde{\omega}_i(t) + \tilde{s}_i(t)$  and  $\nu_i(t) = -s_i(t) \tilde{\omega}_i(t) + \tilde{c}_i(t)$  as two exogenous signals.

For the follower  $i \in \mathcal{V}_B$ , by system (28), we have

$$\begin{aligned} \dot{\tilde{s}}_i &= \omega_r \tilde{c}_i + \sum_{j \in \mathcal{N}_i} a_{ij} (\tilde{s}_j - \tilde{s}_i) \\ \dot{\tilde{c}}_i &= -\omega_r \tilde{s}_i + \sum_{j \in \mathcal{N}_i} a_{ij} (\tilde{c}_j - \tilde{c}_i), \quad i \in \mathcal{V}_B. \end{aligned} \quad (39)$$

For follower  $i$ ,  $i \in \mathcal{V}_A$ , the control law (19) only uses the relative position measurements w.r.t. the leader, and thus, the information of its neighboring followers in  $G$  is not involved in system (38). To describe the actual interaction among multirobot systems, we introduce a subgraph of  $\mathcal{G} = (\mathcal{V}, \mathcal{E}, \mathcal{A})$ , namely  $\underline{\mathcal{G}} = (\mathcal{V}, \underline{\mathcal{E}}, \underline{\mathcal{A}})$ , by removing the directed edges  $(j, i)$ ,  $i \in \mathcal{V}_A$ ,  $j \in \mathcal{V} \setminus \{0, i\}$  from  $\mathcal{E}$ , i.e.,  $\underline{\mathcal{E}} = \mathcal{E} \setminus \{(j, i) : i \in \mathcal{V}_A, j \in \mathcal{V} \setminus \{0, i\}\}$  and  $\underline{\mathcal{A}} = [a_{ij}] \in \mathbb{R}^{N \times N}$  with  $a_{ij} > 0$  if  $(j, i) \in \underline{\mathcal{E}}$  and  $a_{ij} = 0$  otherwise. Since the graph  $\mathcal{G}$  satisfies Assumption 2, the subgraph  $\underline{\mathcal{G}}$  also satisfies Assumption 2. Moreover, for the subgraph  $\underline{\mathcal{G}}$ , we define  $\underline{\mathcal{H}} = \underline{\mathcal{L}} + \underline{\mathcal{B}}$ , where

$\underline{\mathcal{L}}$  is the Laplacian matrix of the subgraph  $\underline{\mathcal{G}}$  and  $\underline{\mathcal{B}} = \text{diag}(b_i)$  with  $b_i = 1$  for  $i \in \mathcal{V}_A$  and  $b_i = 0$  for  $i \in \mathcal{V}_B$ . Then, denote the following stacked vectors,  $\tilde{\mathbf{s}} = [\tilde{s}_1, \dots, \tilde{s}_N]^T \in \mathbb{R}^N$ ,  $\tilde{\mathbf{c}} = [\tilde{c}_1, \dots, \tilde{c}_N]^T \in \mathbb{R}^N$ ,  $\boldsymbol{\mu} = [\mu_1, \dots, \mu_{n_A}, \mathbf{0}_{n_B}^T]^T \in \mathbb{R}^N$ ,  $\boldsymbol{\nu} = [\nu_1, \dots, \nu_{n_A}, \mathbf{0}_{n_B}^T]^T \in \mathbb{R}^N$ , and express the system consisting of (38) and (39) in a compact form as

$$\dot{\tilde{\mathbf{s}}} = \omega_r \tilde{\mathbf{c}} - \underline{\mathcal{H}} \tilde{\mathbf{s}} + \boldsymbol{\mu}(t), \quad \dot{\tilde{\mathbf{c}}} = -\omega_r \tilde{\mathbf{s}} - \underline{\mathcal{H}} \tilde{\mathbf{c}} + \boldsymbol{\nu}(t). \quad (40)$$

Consider the following nominal system:

$$\dot{\tilde{\mathbf{s}}} = \omega_r \tilde{\mathbf{c}} - \underline{\mathcal{H}} \tilde{\mathbf{s}}, \quad \dot{\tilde{\mathbf{c}}} = -\omega_r \tilde{\mathbf{s}} - \underline{\mathcal{H}} \tilde{\mathbf{c}} \quad (41)$$

and  $[\boldsymbol{\mu}^T(t), \boldsymbol{\nu}^T(t)]^T$  can be viewed as a perturbation. Choose a Lyapunov function candidate  $V_{(3)} = \frac{1}{2} \tilde{\mathbf{s}}^T P \tilde{\mathbf{s}} + \frac{1}{2} \tilde{\mathbf{c}}^T P \tilde{\mathbf{c}}$ , where  $P = \text{diag}(e_i/f_i)$  with  $[e_1, \dots, e_{n_B}]^T = \underline{\mathcal{H}} \mathbf{1}_{n_B}$  and  $[f_1, \dots, f_{n_B}]^T = \underline{\mathcal{H}}^{-T} \mathbf{1}_{n_B}$ . Taking the time derivative of  $V_{(3)}$  along the trajectories of system (41) yields

$$\begin{aligned} \dot{V}_{(3)} &= \omega_r \tilde{\mathbf{s}}^T P \tilde{\mathbf{c}} - \omega_r \tilde{\mathbf{c}}^T P \tilde{\mathbf{s}} + \frac{1}{2} \mathbf{s}^T (P \underline{\mathcal{H}} + \underline{\mathcal{H}}^T P) \mathbf{s} \\ &\quad + \mathbf{c}^T (P \underline{\mathcal{H}} + \underline{\mathcal{H}}^T P) \mathbf{c} \leq -\frac{\lambda_{\min}(Q)}{\lambda_{\max}(P)} V_{(3)} \end{aligned} \quad (42)$$

where  $Q = P \underline{\mathcal{H}} + \underline{\mathcal{H}}^T P$  is positive definite by Assumption 2 and Lemma 3. Hence, system (41) is uniformly exponentially stable. Moreover, for robot  $i \in \mathcal{V}_A$ , we have already let  $\hat{s}_i = s_i$ . By Theorem 1, we have  $s_{ei} \rightarrow 0$ , i.e.,  $s_i \rightarrow s_0$ , and then,  $\tilde{s}_i = \hat{s}_i - s_0 = s_i - s_0 \rightarrow 0$  accordingly. By Theorem 1, one could easily obtain  $\tilde{\omega}_i \rightarrow 0$ . It follows from  $\|\boldsymbol{\mu}(t)\| \leq \sum_{i=1}^{n_A} (|c_i| |\tilde{\omega}_i| + |\tilde{s}_i|) \leq \sum_{i=1}^{n_A} (|\tilde{\omega}_i| + |\tilde{s}_i|)$  that  $\boldsymbol{\mu}(t) \rightarrow \mathbf{0}_N$  as  $t \rightarrow \infty$  asymptotically. Similarly, we have  $\boldsymbol{\nu}(t) \rightarrow \mathbf{0}_N$  as  $t \rightarrow \infty$ . Therefore, by Lemma 1(b), system (40) is uniformly asymptotically stable. Consequently, system (39) is also uniformly asymptotically stable.

Second, we show the convergence of  $\tilde{x}_i$  and  $\tilde{y}_i$  for  $i \in \mathcal{V}_A \cup \mathcal{V}_B$ . For the follower  $i \in \mathcal{V}_A$ , it follows from  $\hat{e}_i^x = e_i^x$  and  $\hat{e}_i^y = e_i^y$  that  $\tilde{x}_i \equiv 0$  and  $\tilde{y}_i \equiv 0$ . Accordingly, we write

$$\dot{\tilde{x}}_i \equiv -\tilde{x}_i + \tilde{x}_i, \quad \dot{\tilde{y}}_i \equiv -\tilde{y}_i + \tilde{y}_i, \quad i \in \mathcal{V}_A. \quad (43)$$

For the follower  $i \in \mathcal{V}_B$ , by system (28), we have

$$\begin{aligned} \dot{\tilde{x}}_i &= \sum_{j \in \mathcal{N}_i} a_{ij} (\tilde{x}_j - \tilde{x}_i) + v_r \tilde{c}_i \\ \dot{\tilde{y}}_i &= \sum_{j \in \mathcal{N}_i} a_{ij} (\tilde{y}_j - \tilde{y}_i) + v_r \tilde{s}_i, \quad i \in \mathcal{V}_B. \end{aligned} \quad (44)$$

We denote the stacked vectors  $\tilde{\mathbf{x}} = [\tilde{x}_1, \dots, \tilde{x}_N]^T$  and  $\tilde{\mathbf{y}} = [\tilde{y}_1, \dots, \tilde{y}_N]^T \in \mathbb{R}^N$ , and two exogenous signals  $\boldsymbol{\epsilon}(t) = [\tilde{\mathbf{x}}_A^T, v_r \tilde{\mathbf{c}}_B^T]^T$  and  $\boldsymbol{\nu}(t) = [\tilde{\mathbf{y}}_A^T, v_r \tilde{\mathbf{s}}_B^T]^T$ , where  $\tilde{\mathbf{x}}_A = [\tilde{x}_1, \dots, \tilde{x}_{n_A}]^T$ ,  $\tilde{\mathbf{y}}_A = [\tilde{y}_1, \dots, \tilde{y}_{n_A}]^T$ ,  $\tilde{\mathbf{s}}_B = [\tilde{s}_{n_A+1}, \dots, \tilde{s}_N]^T$ , and  $\tilde{\mathbf{c}}_B = [\tilde{c}_{n_A+1}, \dots, \tilde{c}_N]^T$ . Then, we express the system consisting of (43) and (44) in a compact form as

$$\dot{\tilde{\mathbf{x}}} = -\underline{\mathcal{H}} \tilde{\mathbf{x}} + \boldsymbol{\epsilon}(t), \quad \dot{\tilde{\mathbf{y}}} = -\underline{\mathcal{H}} \tilde{\mathbf{y}} + \boldsymbol{\nu}(t). \quad (45)$$

For follower  $i \in \mathcal{V}_A$ , we have  $\tilde{\mathbf{x}}_A = \mathbf{0}_{n_A}$  and  $\tilde{\mathbf{y}}_A = \mathbf{0}_{n_A}$ . For follower  $i \in \mathcal{V}_B$ , since the system (39) is uniformly asymptotically stable and  $v_r$  is bounded by Assumption 1, both the exogenous signals  $\boldsymbol{\epsilon}(t)$  and  $\boldsymbol{\nu}(t)$  converge to zero as  $t \rightarrow \infty$ . By

a similar analysis as that of system (40) and Lemma 1(b), we can prove that system (45) is uniformly asymptotically stable. Consequently, system (44) is also uniformly asymptotically stable. Therefore,  $\zeta_i(t) = [\tilde{x}_i(t), \tilde{y}_i(t), \tilde{s}_i(t), \tilde{c}_i(t)]^T$  converges to zero asymptotically as  $t \rightarrow \infty$ , that is, the observer (25) makes  $[\hat{e}_i^x, \hat{e}_i^y, \hat{s}_i, \hat{c}_i]^T$  asymptotically converge to  $[e_i^x, e_i^y, s_0, c_0]^T$ . The proof is thus completed. ■

## REFERENCES

- [1] K.-K. Oh, M.-C. Park, and H.-S. Ahn, "A survey of multi-agent formation control," *Automatica*, vol. 53, pp. 424–440, 2015.
- [2] Y. Wang, Y. Yue, M. Shan, L. He, and D. Wang, "Formation reconstruction and trajectory replanning for multi-UAV patrol," *IEEE/ASME Trans. Mechatronics*, vol. 26, no. 2, pp. 719–729, Apr. 2021.
- [3] X. Zhao, B. Tao, and H. Ding, "Multimobile robot cluster system for robot machining of large-scale workpieces," *IEEE/ASME Trans. Mechatronics*, vol. 27, no. 1, pp. 561–571, Feb. 2022.
- [4] K. M. Kabore and S. Güler, "Distributed formation control of drones with onboard perception," *IEEE/ASME Trans. Mechatronics*, vol. 27, no. 5, pp. 3121–3131, Oct. 2022, doi: [10.1109/TMECH.2021.3110660](https://doi.org/10.1109/TMECH.2021.3110660).
- [5] X. Yu and R. Su, "Decentralized circular formation control of nonholonomic mobile robots under a directed sensor graph," *IEEE Trans. Autom. Control*, early access, doi: [10.1109/TAC.2022.3194096](https://doi.org/10.1109/TAC.2022.3194096).
- [6] T. Balch and R. C. Arkin, "Behavior-based formation control for multi-robot teams," *IEEE Trans. Robot. Autom.*, vol. 14, no. 6, pp. 926–939, Dec. 1998.
- [7] A. Ailon and I. Zohar, "Control strategies for driving a group of nonholonomic kinematic mobile robots in formation along a time-parameterized path," *IEEE/ASME Trans. Mechatronics*, vol. 17, no. 2, pp. 326–336, Apr. 2012.
- [8] E. Yang and D. Gu, "Nonlinear formation-keeping and mooring control of multiple autonomous underwater vehicles," *IEEE/ASME Trans. Mechatronics*, vol. 12, no. 2, pp. 164–178, Apr. 2007.
- [9] B. Mu and Y. Shi, "Distributed LQR consensus control for heterogeneous multiagent systems: Theory and experiments," *IEEE/ASME Trans. Mechatronics*, vol. 23, no. 1, pp. 434–443, Feb. 2018.
- [10] K. D. Do, "Bounded assignment formation control of second-order dynamic agents," *IEEE/ASME Trans. Mechatronics*, vol. 19, no. 2, pp. 477–489, Apr. 2014.
- [11] V. P. Tran, F. Santoso, M. Garratt, and I. R. Petersen, "Distributed formation control using fuzzy self-tuning of strictly negative imaginary consensus controllers in aerial robotics," *IEEE/ASME Trans. Mechatronics*, vol. 26, no. 5, pp. 2306–2315, Oct. 2021.
- [12] H. Su, C. Chen, Z. Yang, S. Zhu, and X. Guan, "Bearing-based formation tracking control with time-varying velocity estimation," *IEEE Trans. Cybern.*, early access, doi: [10.1109/TCYB.2022.3169891](https://doi.org/10.1109/TCYB.2022.3169891).
- [13] J. P. Desai, J. P. Ostrowski, and V. Kumar, "Modeling and control of formations of nonholonomic mobile robots," *IEEE Trans. Robot. Autom.*, vol. 17, no. 6, pp. 905–908, Dec. 2001.
- [14] Z. Lin, B. Francis, and M. Maggiore, "Necessary and sufficient graphical conditions for formation control of unicycles," *IEEE Trans. Autom. Control*, vol. 50, no. 1, pp. 121–127, Jan. 2005.
- [15] K. D. Do and J. Pan, "Nonlinear formation control of unicycle-type mobile robots," *Robot. Autom. Syst.*, vol. 55, no. 3, pp. 191–204, 2007.
- [16] N. Léchevin, C. A. Rabbath, and P. Sicard, "Trajectory tracking of leader-follower formations characterized by constant line-of-sight angles," *Automatica*, vol. 42, no. 12, pp. 2131–2141, 2006.
- [17] L. Consolini, F. Morbidi, D. Prattichizzo, and M. Tosques, "Stabilization of a hierarchical formation of unicycle robots with velocity and curvature constraints," *IEEE Trans. Robot.*, vol. 25, no. 5, pp. 1176–1184, Oct. 2009.
- [18] T. Liu and Z.-P. Jiang, "Distributed formation control of nonholonomic mobile robots without global position measurements," *Automatica*, vol. 49, no. 2, pp. 592–600, 2013.
- [19] T. Liu and Z.-P. Jiang, "Distributed nonlinear control of mobile autonomous multi-agents," *Automatica*, vol. 50, no. 4, pp. 1075–1086, 2014.
- [20] X. Yu and L. Liu, "Distributed formation control of nonholonomic vehicles subject to velocity constraints," *IEEE Trans. Ind. Electron.*, vol. 63, no. 2, pp. 1289–1298, Feb. 2016.
- [21] J. Chen, D. Sun, J. Yang, and H. Chen, "Leader-follower formation control of multiple non-holonomic mobile robots incorporating a receding-horizon scheme," *Int. J. Robot. Res.*, vol. 29, no. 6, pp. 727–747, 2010.
- [22] M. Maghenem, A. Loría, and E. Panteley, "Formation-tracking control of autonomous vehicles under relaxed persistency of excitation conditions," *IEEE Trans. Control Syst. Technol.*, vol. 26, no. 5, pp. 1860–1865, Sep. 2018.
- [23] X. Liang, H. Wang, Y.-H. Liu, Z. Liu, and W. Chen, "Leader-following formation control of nonholonomic mobile robots with velocity observers," *IEEE/ASME Trans. Mechatronics*, vol. 25, no. 4, pp. 1747–1755, Aug. 2020.
- [24] S.-G. Kim, J. L. Crassidis, Y. Cheng, A. M. Fosbury, and J. L. Junkins, "Kalman filtering for relative spacecraft attitude and position estimation," *J. Guid. Control Dyn.*, vol. 30, no. 1, pp. 133–143, 2007.
- [25] J. L. Crassidis, F. L. Markley, and Y. Cheng, "Survey of nonlinear attitude estimation methods," *J. Guid. Control Dyn.*, vol. 30, no. 1, pp. 12–28, 2007.
- [26] H. Kannan, V. K. Chitrakaran, D. M. Dawson, and T. Burg, "Vision-based leader/follower tracking for nonholonomic mobile robots," in *Proc. Amer. Control Conf.*, 2007, pp. 2159–2164.
- [27] O. A. Orqueda and R. Fierro, "Robust vision-based nonlinear formation control," in *Proc. Amer. Control Conf.*, 2006, pp. 1422–1427.
- [28] J. Jakubiak, E. Lefeber, K. Tchoń, and H. Nijmeijer, "Two observer-based tracking algorithms for a unicycle mobile robot," *Int. J. Appl. Math. Comput. Sci.*, vol. 12, pp. 513–522, 2002.
- [29] A. Bayuwindra, E. Lefeber, J. Ploeg, and H. Nijmeijer, "Extended look-ahead tracking controller with orientation-error observer for vehicle platooning," *IEEE Trans. Intell. Transp. Syst.*, vol. 21, pp. 4808–4821, Nov. 2020.
- [30] Y. Kanayama, Y. Kimura, F. Miyazaki, and T. Noguchi, "A stable tracking control method for an autonomous mobile robot," in *Proc. IEEE Int. Conf. Robot. Autom.* 1990, pp. 384–389.
- [31] H. K. Khalil, *Nonlinear Systems*, 3rd ed. Hoboken, NJ, USA: Prentice-Hall, 2002.
- [32] H. Zhang, Z. Li, Z. Qu, and F. L. Lewis, "On constructing Lyapunov functions for multi-agent systems," *Automatica*, vol. 58, pp. 39–42, 2015.
- [33] R. Zheng, Y. Liu, and D. Sun, "Enclosing a target by nonholonomic mobile robots with bearing-only measurements," *Automatica*, vol. 53, pp. 400–407, 2015.
- [34] S. Zhao, Z. Li, and Z. Ding, "Bearing-only formation tracking control of multiagent systems," *IEEE Trans. Autom. Control*, vol. 64, no. 11, pp. 4541–4554, Nov. 2019.
- [35] A. D. Ames, X. Xu, J. W. Grizzle, and P. Tabuada, "Control barrier function based quadratic programs for safety critical systems," *IEEE Trans. Autom. Control*, vol. 62, no. 8, pp. 3861–3876, Aug. 2017.



**Jianing Zhao** (Student Member, IEEE) received the B.E. degree in automation from the University of Science and Technology of China, Hefei, China, in 2019. He is currently working toward the Ph.D. degree in control science and engineering, Shanghai Jiao Tong University, Shanghai, China.

His research interests include discrete-event systems, multiagent systems, and mobile robotics.



**Keyi Zhu** received the B.S. degree in mechanical engineering from Shanghai Jiao Tong University, Shanghai, China, in 2021. He will work toward the Ph.D. degree in mechanical engineering with Michigan State University, East Lansing, MI, USA.

His research interests include multiagent systems, mobile robotics, and robotic planning.



**Hanjiang Hu** received the B.Eng. degree in mechanical engineering and the M.S. degree in control science and engineering from Shanghai Jiao Tong University, Shanghai, China, in 2018 and 2021, respectively. He is currently working toward the Ph.D. degree in mechanical engineering with Carnegie Mellon University, Pittsburgh, PA, USA.

His current research interests include visual perception and localization, autonomous driving, multiagent systems, and reinforcement learning.



**Xiao Yu** (Member, IEEE) received the B.S. degree in electrical engineering and automation from Southwest Jiaotong University, Chengdu, China, in 2010, the M.E. degree in control engineering from Xiamen University, Xiamen, China, in 2013, and the Ph.D. degree in mechanical and biomedical engineering from City University of Hong Kong, Hong Kong SAR, China, in 2017.

From 2018 to 2019, he was an Assistant Professor with the Department of Automation,

Shanghai Jiao Tong University, Shanghai, China. He is currently an Associate Professor with the Department of Automation, Xiamen University. His current research interests include multiagent systems, learning-based control, mobile robotics, and complex systems.



**Xianwei Li** (Member, IEEE) received the B.E. degree in automation in 2009 and the M.E. and Ph.D. degrees in control science and engineering in 2011 and 2015, respectively, all from the Harbin Institute of Technology, Harbin, China.

From 2015 to 2019, he was a Research Fellow first with the School of Electrical and Electronic Engineering, Nanyang Technological University, Singapore, and then with the Department of Electrical and Computer Engineering, Technical University of Munich, Munich, Ger-

many. He is currently an Associate Professor with the Department of Automation, Shanghai Jiao Tong University, Shanghai, China. His research interests mainly include multiagent systems, networked control systems, and robust control/filtering.

Dr. Li was a recipient of the Alexander von Humboldt Research Fellowship in 2017 and the CAA Excellent Doctoral Dissertation Award in 2016.



**Hesheng Wang** (Senior Member, IEEE) received the B.Eng. degree in electrical engineering from the Harbin Institute of Technology, Harbin, China, in 2002, and the M.Phil. and Ph.D. degrees in automation and computer-aided engineering from the Chinese University of Hong Kong, Hong Kong SAR, China, in 2004 and 2007, respectively.

He was a Postdoctoral Fellow and a Research Assistant with the Department of Mechanical and Automation Engineering, The Chinese University of Hong Kong, from 2007 to 2009.

He is currently a Professor with the Department of Automation, Shanghai Jiao Tong University, Shanghai, China. His current research interests include visual servoing, service robot, adaptive robot control, and autonomous driving.

Dr. Wang is an Associate Editor for IEEE TRANSACTIONS ON AUTOMATION SCIENCE AND ENGINEERING, IEEE ROBOTICS AND AUTOMATION LETTERS, *Assembly Automation*, and *International Journal of Humanoid Robotics*, a Technical Editor for IEEE/ASME TRANSACTIONS ON MECHATRONICS, and the Editor for the Conference Editorial Board of the IEEE Robotics and Automation Society. He was an Associate Editor for IEEE TRANSACTIONS ON ROBOTICS from 2015 to 2019. He was the General Chair of 2022 IEEE International Conference on Robotics and Biomimetics (ROBIO) and 2016 IEEE International Conference on Real-Time Computing and Robotics and the Program Chair of IEEE ROBIO 2014 and 2019 IEEE/ASME International Conference on Advanced Intelligent Mechatronics. He will be the General Chair of 2025 IEEE/RSJ International Conference on Intelligent Robots and Systems.